THE PARAVENTRICULAR THALAMUS IS A CRITICAL MEDIATOR OF TOP-DOWN CONTROL OF CUE-MOTIVATED BEHAVIOR

*Paolo Campus[a], *Ignacio R. Covelo[a], Youngsoo Kim[b], Aram Parsegian[a], Brittany N. Kuhn[c], Sofia A. Lopez[c], John F. Neumaier[d], Susan M. Ferguson[d], Leah C. Solberg Woods [e], Martin Sarter[b,c], Shelly B. Flagel[a,b,f].

a. Molecular and Behavioral Neuroscience Institute, University of Michigan, Ann Arbor, MI, USA.
b. Department of Psychology, University of Michigan, Ann Arbor, MI, USA.
c. Neuroscience Graduate Program, University of Michigan, Ann Arbor, MI, USA.
d. Department of Psychiatry and Behavioral Sciences, University of Washington, Seattle, WA, USA.
e. Department of Internal Medicine, Molecular Medicine, Center on Diabetes, Obesity and Metabolism, Wake Forest School of Medicine, Winston-Salem, NC, USA
f. Department of Psychiatry, University of Michigan, Ann Arbor, MI, USA.

Corresponding author:

Shelly B. Flagel, Ph.D.
Associate Professor
Department of Psychiatry
Molecular and Behavioral Neuroscience Institute
University of Michigan
Email: sflagel@umich.edu
Phone: 734-936-2033

Short title: THE PARAVENTRICULAR THALAMUS MEDIATES CUE-MOTIVATED BEHAVIOR

Keywords: Incentive salience, prelimbic cortex, paraventricular nucleus of the thalamus, nucleus accumbens, sign-tracking, dopamine

Number of figures in the main text: 5

Number of tables in the main text: 0

Number of figures in the supplemental results: 3

Number of tables in the supplemental results: 6

Abstract

Stimuli or cues in the environment can elicit complex emotional states, and thereby maladaptive behavior, as a function of their ascribed value. Here we capture individual variation in the propensity to attribute motivational value to reward-cues using the sign-tracker/goal-tracker animal model. Goal-trackers attribute predictive value to reward-cues, and sign-trackers attribute both predictive and incentive value. Using chemogenetics and microdialysis, we show that, in sign-trackers, stimulation of the neuronal pathway from the prelimbic cortex (PrL) to the paraventricular nucleus of the thalamus (PVT) decreases the incentive value of a reward-cue. In contrast, in goal-trackers, inhibition of the PrL-PVT pathway increases both the incentive value and dopamine levels in the nucleus accumbens shell. The PrL-PVT pathway, therefore, exerts top-down control over the dopamine-dependent process of incentive salience attribution. These results highlight PrL-PVT pathway as a potential target for treating psychopathologies associated with the attribution of excessive incentive value to reward-cues, including addiction.

Introduction

Learning to associate environmental stimuli with the availability of valuable resources, such as food, is critical for survival. Such stimulus-reward associations rely on Pavlovian conditioning, a learning process during which a once neutral stimulus becomes a conditioned stimulus (CS), as it reliably predicts the delivery of an unconditioned stimulus (US) (e.g. food). The CS, then, attains predictive value and comes to elicit a conditioned response. Yet, we know from both preclinical and clinical studies that CSs can also acquire incentive value and elicit complex emotional and motivational states [1-4]. When a CS is attributed with incentive salience and transformed into an incentive stimulus, it becomes attractive and desirable in its own right. That is, the CS becomes a "motivational magnet", now capable of capturing attention and eliciting approach behavior [5]. However, individuals vary in their propensity to attribute incentive value to reward-cues, and only for some individuals do such cues acquire inordinate control over behavior and the ability to elicit maladaptive tendencies [6,7].

The preferential use of predictive vs. incentive learning strategies reflects distinct cognitive-motivational styles [8] that bias the way an individual responds to reward-cues. While both strategies may be adaptive under the right conditions, an extreme bias for the selective use of a single strategy may contribute to an increased risk for specific pathologies. Indeed, several psychiatric disorders have been associated with excessive attribution of motivational significance to environmental cues, including substance use disorder [9-12], eating disorders [13,14], gambling disorder [15], post-traumatic stress disorder (PTSD) [16], and bipolar disorder [17,18]. On the other side of the spectrum, a deficit in the attribution of incentive value to reward-cues has been associated with avolition (i.e. anticipatory anhedonia), a constitutive symptom of major depressive disorder [18-20]. Notably, the mesocorticolimbic dopamine system, which plays a major role in the attribution of incentive salience to reward-cues [21-23], has been implicated in all of these disorders [18,24-27].

In recent years, an animal model has been established that enables us to parse the neurobiological mechanisms underlying predictive vs. incentive Pavlovian learning. When rats are exposed to a Pavlovian conditioned approach (PavCA) paradigm in which the presentation of a lever-CS is immediately followed by the response-

independent delivery of food-US, distinct conditioned responses emerge. Some rats, goal-trackers (GTs), approach the location of impending food delivery upon the lever-CS presentation, while others, sign-trackers (STs), approach and interact with the lever-CS itself. For both GTs and STs the lever-CS acquires predictive value and elicits a conditioned response, but for STs, the CS also acquires incentive value. This animal model, therefore, provides a unique platform to investigate the neurobiological determinants of individual differences in the propensity to attribute incentive salience to reward-cues.

Previous studies suggest that sign-tracking behavior results from enhanced activity in subcortical brain circuits known to mediate motivated behaviors, including the striatal dopamine system, the amygdala, and the hypothalamus [22,23,28-31]. In addition, relative to GTs, STs appear to have deficits in top-down cognitive control originating in the prefrontal cortex [32]. Thus, we hypothesize that sign-tracking behavior arises from an imbalance between top-down cognitive control and bottom-up motivational processes. One brain region that is ideally situated to act as a fulcrum between cortical, limbic and homeostatic circuits is the paraventricular nucleus of the thalamus (PVT). The PVT has, in fact, come to be known as the “thalamic gateway” [33] for appetitive motivation; acting to integrate cognitive, emotional, motivational and viscerosensitive information, and, in turn, guide behavioral responses [33,34]. Consistent with this view, the PVT has been implicated in the propensity to attribute incentive motivational value to reward-cues [35-37].

The functional connectivity of the PVT in response to cue-induced neuronal activity differentiates STs from GTs [28,29,35]. In STs, cue-induced activity in the PVT is correlated with activity in subcortical areas, including the nucleus accumbens (NAc); whereas in GTs, cue-induced activity in the PVT is correlated with activity in the prelimbic cortex (PrL) [28,35]. Further investigation of PVT-associated circuity in STs and GTs revealed that these phenotypes exhibit the same degree of cue-induced neural activity in PrL neurons that project to the PVT; but STs show greater cue-induced activity in subcortical afferents to the PVT, including the hypothalamus, and efferents from the PVT, including those to the NAc [29]. These data suggest that the predictive value of the reward-cue is encoded in the PrL-PVT circuit. In STs, however, cognitive information about the predictive value of the reward-cue presumably competes with

overriding subcortical motivational circuits, thus rendering them more prone to attribute incentive value. From this, we hypothesized that stimulating the PrL-PVT circuit (i.e. enhancing top-down control) in STs would reduce the tendency to attribute incentive value to a food-cue, by counteracting their inherent bias towards bottom-up/motivational mechanisms. In contrast, we hypothesized that inhibiting the PrL-PVT circuit (i.e. attenuating top-down control) in GTs would increase the tendency to attribute incentive value to a food-cue, by weakening the top-down cognitive component of the system and permitting bottom-up motivational mechanisms to act. Because the PVT sends dense projections to the NAc [34,38,39], and can affect local dopamine (DA) release [40-44], we also hypothesized that manipulations of PrL-PVT activity would affect extracellular DA levels in the NAc shell (NAcS), where PVT connections are most dense [39]. Specifically, we predicted that stimulation of the PrL-PVT circuit in STs would decrease DA in the NAcS, whereas inhibition of the PrL-PVT circuit in GTs would increase DA in the NAcS. To test these hypotheses, we used a dual-vector approach [45-47] to express either the stimulatory Gq- or inhibitory Gi/o- DREADD (Designer Receptors Exclusively Activated by Designer Drugs) in neurons of the PrL that project to the PVT, and examined how bidirectional manipulations of this pathway affect the attribution of incentive salience to a food-cue (Experiment 1). In addition, we used in-vivo microdialysis to assess extracellular levels of DA in the NAcS following manipulations of the PrL-PVT pathway (Experiment 2).

Methods and Materials

Detailed methods are included in the Supplemental Methods and Materials.

Common Methods

Subjects. A total of 428 male heterogeneous stock (N/NIH-HS) rats from the breeding colony at the Medical College of Wisconsin (LSW, now at Wake Forest School of Medicine) were used for Experiment 1. A total of 64 male Sprague-Dawley (Charles River Saint-Constant, Canada and Raleigh, NC, USA) rats were used for Experiment 2.

Viral Vectors. Double-floxed $hM_3D(Gq)$ (AAV5-hSyn-DIO-hM_3Dq-mCherry, titer of 4.8 x 10^{12} vg/µL) or $hM_4D(Gi)$ DREADDs (AAV-hSyn-DIO-hM_4Di-mCherry, titer of 1.9 to 2.5 x

10^{13} vg/μL) were obtained from the University of North Carolina vector core. Canine adenovirus expressing Cre (CAV2-Cre, titer of ~ 2.5 x 10^9 vg/μL) was obtained from Dr. Neumaier at the University of Washington.

Drugs. Clozapine-N-oxide (CNO) was obtained from the National Institute of Mental Health (NIMH). CNO was dissolved in 6% dimethylsulfoxide (DMSO) in sterile water and administered intraperitoneally (i.p.) at a dose of 3.0 mg/kg. A 6% DMSO solution in sterile water was used as the vehicle (VEH) control.

Pavlovian conditioned approach. The Pavlovian conditioned approach (PavCA) apparatus and procedures were the same as those described previously [48,49]. Briefly, the presentation of an illuminated lever-CS preceded the non-contingent delivery of a food pellet (US) into an adjacent food cup, and 25 lever-food pairings occurred per session. Behavior directed towards either the lever-CS (i.e. sign-tracking) or food cup (i.e. goal-tracking) were assessed.

Surgery. For both Experiments 1 and 2, Cre-dependent DREADD viruses (Gq or Gi) were bilaterally injected into the PrL (from bregma: +3.0 mm AP; ±1.0 mm ML; -4 mm DV) at a rate of 200 nL per minute over a 5-min period (1 μL total). CAV2-Cre was injected at a 10° angle into the aPVT (from bregma: -2.0 mm AP; -1 mm ML; -5.4 mm DV) and pPVT (from bregma: -3.0 mm AP; -1 mm ML; -5.5 mm DV) at a rate of 50 nL per minute for 2 minutes (100 nL total volume). Following delivery, injectors were left in place for an additional 5 minutes to allow diffusion. For Experiment 2, rats were additionally implanted with a guide cannula (CMA 12, Harvard Apparatus, Holliston, MA), counterbalanced in the left or right NAcS (from bregma: +1.3 mm AP; ±0.8 mm ML; -5.2 mm DV). Cannulas were secured to the skull with stainless steel screws and acrylic cement (Bosworth New Truliner, Keystone Industries, Gibbstown, NJ). Removable stylets were placed in the guide cannulas to avoid clogging. Behavioral tests were conducted 3-5 weeks following surgery.

Immunohistochemistry. Brain fixation, tissue processing and immunohistochemistry were performed using standard methods as previously described [29], and modified as described in the Supplemental Methods and Materials.

Statistical analyses. Statistical analyses are described in detail in the Supplemental Methods and Materials. Data with repeated measures were analyzed using a linear mixed-effects model (LMM). All other data were analyzed using analysis of variance (ANOVA) or an unpaired t-test. The relationship between variables was also assessed using regression analysis. Data were analyzed independently for each phenotype and G protein-coupled receptor (GPCR) (i.e. Gq, Gi or no-DREADD), as the studies occurred at different times and the hypotheses to be tested did not call for comparison between Phenotypes or type of GPCR. All statistical analyses were performed using IBM SPSS Statistics 24 (IBM, Armonk, NY, USA). Alpha was set at 0.05. When significant interactions were detected, Bonferroni post-hoc comparisons were performed. Effect sizes for pairwise comparisons were calculated using Cohen's d [50], as previously reported [48]. Effect sizes <0.2 were considered "small", effects sizes ≥0.2≤0.8 were considered "medium", and effect sizes >0.8 were considered large [50,51].

Experiment 1 Methods

PavCA rescreening and test. The experimental design for Experiment 1 is summarized in Figure 1a. Following recovery from surgery and DREADD incubation, rats underwent 5 PavCA rescreening sessions (sessions 6-10) to determine if their initial behavioral characterization as a ST or GT had changed. To habituate rats to the injection procedures, all rats received an injection (i.p.) of vehicle 25 minutes prior to session 10. The PavCA testing phase occurred during sessions 11-16, and rats received administration of CNO or VEH 25 minutes prior to each session.

Conditioned reinforcement test. The day after the completion of PavCA training, rats were exposed to a conditioned reinforcement test (CRT) as described previously [48]. Briefly, responses into a port designated 'active' resulted in the brief presentation of the lever-CS (in the absence of food reward). The incentive value index [48] (active nose pokes + lever presses – inactive nose pokes) was calculated to capture all of the behavioral measures obtained during the conditioned reinforcement test.

Experiment 2 Methods

PavCA training. The experimental design for Experiment 2 is summarized in Figure 5a-f. PavCA training apparatus and experimental procedures were the same as described above and in the Supplemental Methods and Materials [48,49]. During all PavCA training sessions rats were tethered to a swivel arm to habituate them to the microdialysis procedures. In this experiment, rats were phenotyped as STs or GTs following 3 initial PavCA sessions [52], and subsequently received CNO or VEH 25 minutes prior to the remaining PavCA training sessions (sessions 4-6).

Microdialysis. Microdialysis methods are depicted in Fig. 5f. Extracellular levels of neurotransmitters in the NAc shell were assessed during session 6 of PavCA training. The percentage change from baseline was measured for the following neurotransmitters: GABA, glutatmate (Glu), dopamine (DA), serotonin (5-HT) and acetylcholine (Ach). Briefly, before session 6 of PavCA training, microdialysis probes were inserted in the NAcS. Dialysate samples (5 μl) were collected every 5 minutes, beginning 120 minutes after inserting the probes. Baseline samples were collected for 30 minutes (6 fractions). After this time rats were injected with CNO/VEH and samples were collected for an additional 25 minutes (5 fractions). PavCA training started 25 minutes after CNO/VEH injections. Samples were collected during the PavCA session for a total time of 35 minutes (PavCA samples, 7 fractions). After collection, samples were derivatized and analyzed using high-performance liquid chromatography-tandem mass spectrometry (HPLC-MS) as described previously [53].

Results

Experiment 1

Acquisition of Pavlovian conditioned approach behaviors.

The average PavCA index from sessions 4-5 was used to classify rats as STs (PavCA index ≥ +0.30) or GTs (PavCA index ≤ -0.30) (Fig. 2b). Linear mixed-effects models showed a significant effect of phenotype, session and a significant phenotype x session interaction for all measure of sign- and goal-tracking behavior. Relative to GTs, STs showed a greater number of lever contacts ($F_{4,159.662}$=58.311, p< 0.001), a greater

probability to contact the lever ($F_{4,274.796}$=67.329, p< 0.001) and had a lower latency to approach the lever ($F_{4,308.710}$=63.970, p<0.001) (Fig. 2c-e). These significant differences were apparent from session 1-5 of PavCA training (post-hoc analyses, P<0.001). In contrast, relative to STs, GTs showed a greater number of magazine entries ($F_{4,226.006}$=53.600, p<0.001), a greater probability to enter the magazine ($F_{4,300.478}$=72.795, p<0.001) and a lower latency to enter the magazine ($F_{4,318.266}$=69.356, p<0.001) (Fig. 2f-h). These significant differences were apparent from PavCA sessions 2-5 (post-hoc analyses, p<0.05) for all measures.

Experimental groups were counterbalanced based on the average PavCA index from sessions 4-5. Rats with a PavCA index between -0.3 and +0.3 (intermediate rats, n=182), rats that changed phenotype before testing (n=55), and rats with inadequate DREADD expression (n=65) were excluded from the remainder of Experiment 1, resulting in a final n=126 (GT-Gi=35, GT-Gq=12, ST-Gi=17, ST-Gq=27, GT-no DREADD=17, ST-no DREADD=18). Nonetheless, as shown in Figure 2i, experimental groups remained balanced. That is, there was a significant effect of phenotype ($F_{1,114}$=2757.513, p<0.001) on PavCA index (Fig 2i), but no significant effects of GPCR or treatment groups, and no significant interactions (see also Supplemental Tables 1 and 2).

PavCA rescreening vs. PavCA test

PavCA index is presented as the primary dependent variable in the main text, but analyses for other dependent variables including, contacts, probability and latency directed towards either the lever-CS or food magazine are included in Supplemental Table S3 and S4.

Stimulation of the PrL-PVT pathway attenuates the incentive value of the food cue in STs, but not in GTs. Stimulation of the PrL-PVT pathway in STs significantly decreased the PavCA index (Fig 3c), which, in this case, is reflective of a decrease in lever-directed behavior (Table S3) and an increase in goal-directed behavior (Table S4). There was a significant effect of treatment ($F_{1,23}$=33.251, p<0.001), session ($F_{1,23}$=10,799, p<0.05), and a significant treatment x session interaction ($F_{1,23}$=14.051, p<0.05) on the PavCA index. Post-hoc analyses revealed a significant difference

between VEH- and CNO-treated STs during both rescreening ($p<0.05$, Cohen's d=1.27) and test ($p<0.001$, Cohen's d=2.74), but only the CNO-treated rats exhibited a change in behavior during the test sessions relative to rescreening ($p<0.001$, Cohen's d=1.18). There was no effect of this manipulation in GTs (Fig 3d). Thus, "turning on" the top-down PrL-PVT circuit appears to selectively attenuate the incentive value of the cue in STs.

Inhibition of the PrL-PVT pathway increases the incentive value of the food cue in GTs, without affecting STs. Inhibition of the PrL-PVT pathway in GTs significantly increased the PavCA index (Fig. 3f). There was a significant effect of treatment ($F_{1,30}$=5.975, $p<0.05$), session ($F_{1,30}$=7.106, $p<0.05$), and a significant treatment x session interaction ($F_{1,30}$=4.403, $p<0.05$). Post-hoc analyses revealed that inhibiting the PrL-PVT pathway increased the PavCA index relative to both the rescreening session ($p<0.05$, Cohen's d=0.85) and to VEH controls during the test session ($p<0.05$, Cohen's d=0.96). There was no effect of this manipulation in STs (Fig 3e), suggesting that "turning off" the PrL-PVT pathway permits the attribution of incentive motivational value to a reward-cue selectively in GTs.

CNO administration in the absence of DREADD receptors does not affect the Pavlovian conditioned approach response in STs or GTs. Administration of CNO in the absence of DREADD had no effect on behavior during PavCA in either STs or GTs (Fig 3g and h, respectively).

Conditioned reinforcement test

The incentive value index is presented as the primary dependent variable in the main text, but analyses for nosepokes and lever contacts are included in the Supplemental Results and in Fig S2.

Stimulation of the PrL-PVT pathway attenuates the conditioned reinforcing properties of a reward-cue in STs, but not GTs. Stimulation of the PrL-PVT pathway in STs significantly attenuated the incentive value index during CRT (t_{25} =-3.574, $p<0.05$, Cohen's d=1.48, Fig. 4b). The same manipulation had no effect in GTs (Fig. 4c). These data are consistent with those reported above for PavCA behavior, as

“turning on” this top-down control attenuates the incentive value of a food-cue selectively in STs.

Inhibition of the PrL-PVT pathway does not affect the conditioned reinforcing properties of a reward-cue in either STs or GTs. Inhibition of the PrL-PVT pathway did not affect the incentive value index during CRT in either STs (Fig. 4d) or GTs (Fig. 4e). Potential explanations for the seemingly incongruent effects of PrL-PVT inhibition on Pavlovian conditioned approach behavior and the conditioned reinforcing properties of the reward-cue in GT are discussed below.

CNO administration in the absence of DREADD receptors does not affect the conditioned reinforcing properties of a reward-cue in STs or GTs. Administration of CNO in the absence of DREADD did not affect the incentive value index during CRT either STs (Fig. 4f) or GTs (Fig. 4g).

Experiment 2

Acquisition of Pavlovian conditioned approach.

Based on the results of Experiment 1, Experiment 2 focused on STs expressing Gq DREADD and GTs expressing Gi DREADD. For this Experiment, the PavCA index from session 3 was used to classify rats as STs and GTs and, since a conditioned response is not fully developed by session 3, different criteria were used for classification. Rats with a PavCA index ≥ +0.20 were classified as STs, and rats with a score ≤ -0.20 were classified as GTs (Fig 5g). Acquisition of sign- and goal-tracking behaviors across sessions 1-3 of PavCA training is reported in Supplemental Tables S5-6. Intermediate rats with a PavCA index between -0.2 and +0.2 (n=18) were excluded from the remainder of Experiment 2, and subjects with inaccurate DREADD expression and/or with incorrect microdialysis probe placement (n=23) were excluded from the statistical analyses, resulting in a final number of 23 rats (GT-Gi=10, ST-Gq=13).

Stimulation of the PrL-PVT pathway does not affect the attribution of incentive value to a food cue or NAcS neurochemistry in STs. Stimulating the PrL-PVT pathway in STs did not affect behavior early in PavCA training (Fig. 5h). These findings

suggest that the PrL-PVT pathway mediates the incentive value of a food-cue once the sign-tracking response is acquired, and not during the acquisition process.

There was not a significant effect of treatment (CNO, VEH), time (5-min bins), nor a significant interaction for any of the molecules examined in the NAc shell (Fig 5j). Noteworthy, however, is a visible trend for DA (Fig. 5k), suggesting that stimulation of the PrL-PVT pathway in STs decreases DA in the NAc shell (p=0.153, Cohen's d=1.26). Yet, consistent with the fact that there were no significant behavioral effects in STs following the same manipulation, there was also not a significant correlation between average DA and PavCA index (Fig. 5l).

Inhibition of the PrL-PVT pathway increases the propensity to attribute incentive value to a food cue and DA levels in the NAcS in GTs. In GTs, inhibiting the PrL-PVT pathway early in training resulted in an enhancement of the incentive motivational value of the reward-cue (effect of treatment ($F_{1,8}$=10.722, p<0.05); treatment x session interaction ($F_{1,8}$=7.163, p<0.05; Fig. 5i)). Post-hoc analysis revealed that CNO treatment significantly increased the PavCA index relative to session 3 (p<0.05, Cohen's d=2.40), and relative to VEH-treated rats on session 6 (p<0.05, Cohen's d=1.94). Thus, inhibition of the PrL-PVT circuit early in training enhances the incentive motivational value of a reward-cue in GTs.

While GABA, Glu, 5-HT and Ach did not differ as a function of treatment or time in GTs (Fig. 5m), DA did (effect of treatment ($F_{1,9.067}$ =11.145, p<0.05); treatment x time interaction ($F_{6,50.149}$ =3.765, p<0.05)). Relative to VEH-treated rats, CNO treatment resulted in a significant increase in extracellular levels of dopamine across the time-sampling period (Fig. 5m); and the same pattern was evident when the average levels of DA were compared (t_8 =2.925, p<0.05, Cohen's d=1.90, Fig. 5n). Thus, in GTs, inhibition of the PrL-PVT circuit increases sign-tracking behavior and concomitantly increases DA in the NAcS. Furthermore, there was a significant positive correlation between percent change in DA and PavCA index ($F_{1,9}$ =91.563, p<0.001; r^2 =0.92), suggesting that DA accounts for more than 90% of the variance in behavior (Fig. 5o).

Discussion

The work presented here highlights the PVT as a central node in the integration of top-down and bottom-up circuits involved in the attribution of incentive motivational value to a Pavlovian food-cue. Specifically, we tested the hypothesis that the PrL-PVT circuit serves to suppress the propensity to attribute incentive value to Pavlovian reward-cues, and that the efficacy of this mechanism is dependent on individual differences in cue-motivated behavior. In support, we found that "turning on" the PrL-PVT pathway via chemogenetic stimulation attenuates the incentive motivational value of a food-cue in sign-tracking rats—those that exhibit a natural propensity to attribute excessive incentive motivational value to such cues—without affecting the behavior of goal-tracking rats. Conversely, "turning off" the PrL-PVT pathway via chemogenetic inhibition appears to permit the attribution of incentive motivational value to reward-cues in GTs, without affecting the behavior of STs.

The current data are consistent with the notion that, in STs, hyper-activation of bottom-up motivational circuits projecting to the PVT override the top-down cognitive information coming from the PrL [29], thus rendering these individuals more prone to attribute incentive value to a food-paired cue. Here we show that this configuration can be altered with stimulation of the PrL-PVT pathway which, presumably, via the PVT, attenuates subcortical drive and updates the behavioral output, resulting in a reduction in sign-tracking behavior. Such an interpretation also explains the lack of effects observed in STs expressing Gi in the PrL-PVT pathway. In these rats, inhibition of the PrL-PVT pathway is without effect because the relative predominance of bottom-up processes remains intact. In contrast, in GTs, top-down processes appear to dominate over subcortical processes [29,32,52]. As a result, GTs are more goal-driven and more inclined to attribute predictive, but not incentive, value to reward-cues. Thus, inhibition of the PrL-PVT pathway in GTs minimizes the top-down control of the PVT, permitting bottom-up signals to gain a relatively greater influence over their behavior. As a result of this shift in balance, GTs show an increase in the expression of sign-tracking behavior. Correspondingly, stimulation of the PrL-PVT pathway in GTs is without effect, as this manipulation merely reinforces the innate top-down control over behavior in these individuals.

For STs, a discrete food-associated cue is able to elicit approach behavior and support the learning of a new instrumental response, or act as a potent conditioned reinforcer [2,49]. Thus, we wanted to determine if the PrL-PVT pathway plays a role in the ability of a food-cue to act as a conditioned reinforcer [2,5]. Although different neural mechanisms are known to contribute to Pavlovian conditioned approach behavior and the conditioned reinforcing effects of Pavlovian cues [54], the PrL-PVT pathway appears to play a prominent role in both, at least for STs. That is, in STs, stimulation of the PrL-PVT circuit reduces both sign-tracking behavior and the conditioned reinforcing properties of the reward-cue. In GTs, however, inhibition of the PrL-PVT pathway did not affect responding during a test of conditioned reinforcement. Although these findings may seem inconsistent with the increase in sign-tracking behavior following this manipulation in GTs, it is important to note that "turning off" this top down control did not switch the behavioral phenotype of GTs to STs. In fact, there was only a moderate increase in the PavCA index. Thus, while inactivation of the PrL-PVT pathway permits the attribution of incentive value to the cue to the extent that it elicits sign-tracking behavior in GTs, the ascribed value is not sufficient to support conditioned reinforcement.

As sign-tracking, but not goal-tracking, behavior is dopamine-dependent, we were also interested in determining whether the chemogenetic manipulations that altered behavior would also affect extracellular levels of DA in the NAc. To this end, we assessed the effects of stimulation (in STs) or inhibition (in GTs) of the PrL-PVT pathway on the neurochemical profile of the NAcS, a subregion of the ventral striatum particularly rich in glutamatergic fibers coming from the PVT [39,55]. For these studies, the effects of PrL-PVT manipulation were examined early in Pavlovian training, when Pavlovian cues are known to evoke a DA response in the NAc to a different degree in STs and GTs [28,56]. Although we expected to observe more robust behavioral effects during this period, we found that stimulation of the PrL-PVT pathway early in Pavlovian training did not affect the behavior of STs, nor did it significantly affect extracellular levels of DA or other neurotransmitters in the NAcS. In contrast, inhibition of the PrL-PVT pathway early in Pavlovian training increased the tendency to sign-track in GTs, and concomitantly increased extracellular levels of DA in the NAcS, without affecting

other neurotransmitters. Thus, in STs, the effects of PrL-PVT stimulation are apparent only after extended Pavlovian conditioning (i.e. Experiment 1); whereas, in GTs, the effects of PrL-PVT inhibition are consistent during early and late stages of Pavlovian conditioning (i.e. in both Experiment 1 and 2). One possible interpretation for these results is that the contribution of bottom-up processes in STs may be more extreme earlier in training, when the sign-tracking response is still being acquired, compared to that after extended training [56]. Therefore, potentiating the top-down communication between the PrL and the PVT during early training may not be strong enough to overcome the subcortical activity surrounding the PVT in STs during this “critical period” of incentive learning. In contrast, the increase in sign-tracking behavior after inhibition of the PrL-PVT pathway in GTs is indeed more pronounced during the early stages of training rather than after prolonged training. It seems, therefore, that a shift towards bottom-up processing during the early stages of Pavlovian training will lead to dopamine-dependent incentive learning. These findings suggest that the PVT acts as a fulcrum in this regard, and that the predominance of bottom-up processes can occur via innate mechanisms (i.e. in STs) or by “turning off” top-down control mechanisms (i.e. in GTs). Ongoing studies will determine whether chemogenetic or optogenetic manipulations of bottom-up processes can similarly alter individual differences in cue-motivated learning strategies.

It has become increasingly apparent in recent years that the PVT and its associated circuitry play an important role in motivated behaviors, including those related to addiction and anxiety-related disorders [16,33,57-68]. Here, we honed in on the PrL-PVT pathway and exploited an animal model of individual differences in cue-reward learning to demonstrate that this circuit acts as a top-down control mechanism to suppress the attribution of incentive value to a food-paired cue. Furthermore, we showed that it does so by affecting the concomitant subcortical processes that instead promote incentive learning, such as DA release in the NAcS. Taken together, these findings identify the PVT as a central node in the integration of top-down and bottom-up mechanisms involved in the attribution of incentive value to reward-cues. The cortico-thalamic-striatal circuitry elucidated here should be considered as a possible target for

new therapeutic interventions to prevent the development of, or treat, cue-motivated psychiatric disorders in vulnerable individuals.

Acknowledgements

Funding for this work was provided by the National Institute on Drug Abuse (NIDA) branch of the National Institutes of Health: R01-DA038599 (SBF), T32-DA007821 (BNK, SAL) and T32-DA007268 (IRC, AP). We would like to acknowledge the technical assistance of Katie Long, Marin Klumpner and Maurice Chojecki throughout the course of these experiments. In addition, we would like to thank Katie Holl for maintenance of the heterogenous stock rat colony at the Medical College of Wisconsin, and Matthew Folz for assistance with confocal imaging in the Molecular and Behavioral Neuroscience Institute at the University of Michigan. We would also like to acknowledge the Flagel Lab members who helped build the foundation for this work, including Dr. Joshua Haight and Kurt Fraser.

References

1 Robinson, T. E. & Berridge, K. C. Review. The incentive sensitization theory of addiction: some current issues. *Philos Trans R Soc Lond B Biol Sci* **363**, 3137-3146, doi:10.1098/rstb.2008.0093 (2008).

2 Robinson, T. E. & Flagel, S. B. Dissociating the predictive and incentive motivational properties of reward-related cues through the study of individual differences. *Biol Psychiatry* **65**, 869-873, doi:10.1016/j.biopsych.2008.09.006 (2009).

3 Pool, E., Sennwald, V., Delplanque, S., Brosch, T. & Sander, D. Measuring wanting and liking from animals to humans: A systematic review. *Neurosci Biobehav Rev* **63**, 124-142, doi:10.1016/j.neubiorev.2016.01.006 (2016).

4 Tibboel, H., De Houwer, J. & Van Bockstaele, B. Implicit measures of "wanting" and "liking" in humans. *Neurosci Biobehav Rev* **57**, 350-364, doi:10.1016/j.neubiorev.2015.09.015 (2015).

5 Berridge, K. C., Robinson, T. E. & Aldridge, J. W. Dissecting components of reward: 'liking', 'wanting', and learning. *Curr Opin Pharmacol* **9**, 65-73, doi:10.1016/j.coph.2008.12.014 (2009).

6 Flagel, S. B., Akil, H. & Robinson, T. E. Individual differences in the attribution of incentive salience to reward-related cues: Implications for addiction. *Neuropharmacology* **56 Suppl 1**, 139-148, doi:10.1016/j.neuropharm.2008.06.027 (2009).

7 Flagel, S. B., Watson, S. J., Robinson, T. E. & Akil, H. Individual differences in the propensity to approach signals vs goals promote different adaptations in the dopamine system of rats. *Psychopharmacology (Berl)* **191**, 599-607, doi:10.1007/s00213-006-0535-8 (2007).

8 Sarter, M. & Phillips, K. B. The neuroscience of cognitive-motivational styles: Sign- and goal-trackers as animal models. *Behav Neurosci* **132**, 1-12, doi:10.1037/bne0000226 (2018).

9 Robinson, T. E. & Berridge, K. C. The neural basis of drug craving: an incentive-sensitization theory of addiction. *Brain Res Brain Res Rev* **18**, 247-291 (1993).

10 Berridge, K. C. & Robinson, T. E. Liking, wanting, and the incentive-sensitization theory of addiction. *Am Psychol* **71**, 670-679, doi:10.1037/amp0000059 (2016).

11 Kwako, L. E. *et al.* Addictions Neuroclinical Assessment: A reverse translational approach. *Neuropharmacology* **122**, 254-264, doi:10.1016/j.neuropharm.2017.03.006 (2017).

12 MacNiven, K. H. *et al.* Association of Neural Responses to Drug Cues With Subsequent Relapse to Stimulant Use. *JAMA Netw Open* **1**, e186466, doi:10.1001/jamanetworkopen.2018.6466 (2018).

13 Berridge, K. C. 'Liking' and 'wanting' food rewards: brain substrates and roles in eating disorders. *Physiol Behav* **97**, 537-550, doi:10.1016/j.physbeh.2009.02.044 (2009).

14 Robinson, M. J. F., Robinson, T. E. & Berridge, K. C. Incentive Salience in Addiction and Over-Consumption. *Interdisciplinary Science of Consumption*, 185-197 (2014).

15 Limbrick-Oldfield, E. H. *et al.* Neural substrates of cue reactivity and craving in gambling disorder. *Transl Psychiatry* **7**, e992, doi:10.1038/tp.2016.256 (2017).

16 Coffey, S. F. *et al.* Craving and physiological reactivity to trauma and alcohol cues in posttraumatic stress disorder and alcohol dependence. *Exp Clin Psychopharmacol* **18**, 340-349, doi:10.1037/a0019790 (2010).
17 Mason, L., O'Sullivan, N., Blackburn, M., Bentall, R. & El-Deredy, W. I want it now! Neural correlates of hypersensitivity to immediate reward in hypomania. *Biol Psychiatry* **71**, 530-537, doi:10.1016/j.biopsych.2011.10.008 (2012).
18 Whitton, A. E., Treadway, M. T. & Pizzagalli, D. A. Reward processing dysfunction in major depression, bipolar disorder and schizophrenia. *Curr Opin Psychiatry* **28**, 7-12, doi:10.1097/YCO.0000000000000122 (2015).
19 Brailean, A. M., Koster, E. H., Hoorelbeke, K. & De Raedt, R. Attentional modulation by reward and punishment cues in relation to depressive symptoms. *J Behav Ther Exp Psychiatry* **45**, 351-359, doi:10.1016/j.jbtep.2014.03.003 (2014).
20 Ubl, B. *et al.* Altered neural reward and loss processing and prediction error signalling in depression. *Soc Cogn Affect Neurosci* **10**, 1102-1112, doi:10.1093/scan/nsu158 (2015).
21 Berridge, K. C. & Robinson, T. E. What is the role of dopamine in reward: hedonic impact, reward learning, or incentive salience? *Brain Res Brain Res Rev* **28**, 309-369 (1998).
22 Flagel, S. B. *et al.* A selective role for dopamine in stimulus-reward learning. *Nature* **469**, 53-57, doi:10.1038/nature09588 (2011).
23 Saunders, B. T. & Robinson, T. E. The role of dopamine in the accumbens core in the expression of Pavlovian-conditioned responses. *The European journal of neuroscience* **36**, 2521-2532, doi:10.1111/j.1460-9568.2012.08217.x (2012).
24 Hamilton, J. P. *et al.* Striatal dopamine deficits predict reductions in striatal functional connectivity in major depression: a concurrent (11)C-raclopride positron emission tomography and functional magnetic resonance imaging investigation. *Transl Psychiatry* **8**, 264, doi:10.1038/s41398-018-0316-2 (2018).
25 Howes, O. D. & Kapur, S. The dopamine hypothesis of schizophrenia: version III--the final common pathway. *Schizophr Bull* **35**, 549-562, doi:10.1093/schbul/sbp006 (2009).
26 Solinas, M., Belujon, P., Fernagut, P. O., Jaber, M. & Thiriet, N. Dopamine and addiction: what have we learned from 40 years of research. *J Neural Transm (Vienna)*, doi:10.1007/s00702-018-1957-2 (2018).
27 Volkow, N. D., Wise, R. A. & Baler, R. The dopamine motive system: implications for drug and food addiction. *Nat Rev Neurosci* **18**, 741-752, doi:10.1038/nrn.2017.130 (2017).
28 Flagel, S. B. *et al.* A food predictive cue must be attributed with incentive salience for it to induce c-fos mRNA expression in cortico-striatal-thalamic brain regions. *Neuroscience* **196**, 80-96, doi:10.1016/j.neuroscience.2011.09.004 (2011).
29 Haight, J. L., Fuller, Z. L., Fraser, K. M. & Flagel, S. B. A food-predictive cue attributed with incentive salience engages subcortical afferents and efferents of the paraventricular nucleus of the thalamus. *Neuroscience* **340**, 135-152, doi:10.1016/j.neuroscience.2016.10.043 (2017).

30 Yager, L. M., Pitchers, K. K., Flagel, S. B. & Robinson, T. E. Individual variation in the motivational and neurobiological effects of an opioid cue. *Neuropsychopharmacology : official publication of the American College of Neuropsychopharmacology* **40**, 1269-1277, doi:10.1038/npp.2014.314 (2015).
31 Singer, B. F. *et al.* Individual variation in incentive salience attribution and accumbens dopamine transporter expression and function. *The European journal of neuroscience* **43**, 662-670, doi:10.1111/ejn.13134 (2016).
32 Paolone, G., Angelakos, C. C., Meyer, P. J., Robinson, T. E. & Sarter, M. Cholinergic control over attention in rats prone to attribute incentive salience to reward cues. *J Neurosci* **33**, 8321-8335, doi:10.1523/JNEUROSCI.0709-13.2013 (2013).
33 Millan, E. Z., Ong, Z. & McNally, G. P. Paraventricular thalamus: Gateway to feeding, appetitive motivation, and drug addiction. *Prog Brain Res* **235**, 113-137, doi:10.1016/bs.pbr.2017.07.006 (2017).
34 Kirouac, G. J. Placing the paraventricular nucleus of the thalamus within the brain circuits that control behavior. *Neurosci Biobehav Rev* **56**, 315-329, doi:10.1016/j.neubiorev.2015.08.005 (2015).
35 Haight, J. L. & Flagel, S. B. A potential role for the paraventricular nucleus of the thalamus in mediating individual variation in Pavlovian conditioned responses. *Front Behav Neurosci* **8**, 79, doi:10.3389/fnbeh.2014.00079 (2014).
36 Haight, J. L., Fraser, K. M., Akil, H. & Flagel, S. B. Lesions of the paraventricular nucleus of the thalamus differentially affect sign- and goal-tracking conditioned responses. *The European journal of neuroscience* **42**, 2478-2488, doi:10.1111/ejn.13031 (2015).
37 Kuhn, B. N., Klumpner, M. S., Covelo, I. R., Campus, P. & Flagel, S. B. Transient inactivation of the paraventricular nucleus of the thalamus enhances cue-induced reinstatement in goal-trackers, but not sign-trackers. *Psychopharmacology (Berl)* **235**, 999-1014, doi:10.1007/s00213-017-4816-1 (2018).
38 Berendse, H. W. & Groenewegen, H. J. Organization of the thalamostriatal projections in the rat, with special emphasis on the ventral striatum. *J Comp Neurol* **299**, 187-228, doi:10.1002/cne.902990206 (1990).
39 Li, S. & Kirouac, G. J. Projections from the paraventricular nucleus of the thalamus to the forebrain, with special emphasis on the extended amygdala. *J Comp Neurol* **506**, 263-287, doi:10.1002/cne.21502 (2008).
40 Choi, D. L. *et al.* Orexin signaling in the paraventricular thalamic nucleus modulates mesolimbic dopamine and hedonic feeding in the rat. *Neuroscience* **210**, 243-248, doi:10.1016/j.neuroscience.2012.02.036 (2012).
41 Jones, M. W., Kilpatrick, I. C. & Phillipson, O. T. Regulation of dopamine function in the nucleus accumbens of the rat by the thalamic paraventricular nucleus and adjacent midline nuclei. *Exp Brain Res* **76**, 572-580 (1989).
42 Parsons, M. P., Li, S. & Kirouac, G. J. Functional and anatomical connection between the paraventricular nucleus of the thalamus and dopamine fibers of the nucleus accumbens. *J Comp Neurol* **500**, 1050-1063, doi:10.1002/cne.21224 (2007).

43 Perez, S. M. & Lodge, D. J. Convergent Inputs from the Hippocampus and Thalamus to the Nucleus Accumbens Regulate Dopamine Neuron Activity. *J Neurosci* **38**, 10607-10618, doi:10.1523/JNEUROSCI.2629-16.2018 (2018).
44 Pinto, A., Jankowski, M. & Sesack, S. R. Projections from the paraventricular nucleus of the thalamus to the rat prefrontal cortex and nucleus accumbens shell: ultrastructural characteristics and spatial relationships with dopamine afferents. *J Comp Neurol* **459**, 142-155, doi:10.1002/cne.10596 (2003).
45 Boender, A. J. *et al.* Combined use of the canine adenovirus-2 and DREADD-technology to activate specific neural pathways in vivo. *PloS one* **9**, e95392, doi:10.1371/journal.pone.0095392 (2014).
46 Kerstetter, K. A. *et al.* Corticostriatal Afferents Modulate Responsiveness to Psychostimulant Drugs and Drug-Associated Stimuli. *Neuropsychopharmacology : official publication of the American College of Neuropsychopharmacology* **41**, 1128-1137, doi:10.1038/npp.2015.253 (2016).
47 Soudais, C., Laplace-Builhe, C., Kissa, K. & Kremer, E. J. Preferential transduction of neurons by canine adenovirus vectors and their efficient retrograde transport in vivo. *FASEB journal : official publication of the Federation of American Societies for Experimental Biology* **15**, 2283-2285, doi:10.1096/fj.01-0321fje (2001).
48 Hughson, A. R. *et al.* Incentive salience attribution, "sensation-seeking" and "novelty-seeking" are independent traits in a large sample of male and female heterogeneous stock rats. *Sci Rep* **9**, 2351, doi:10.1038/s41598-019-39519-1 (2019).
49 Meyer, P. J. *et al.* Quantifying individual variation in the propensity to attribute incentive salience to reward cues. *PloS one* **7**, e38987, doi:10.1371/journal.pone.0038987 (2012).
50 Cohen, J. *Statistical power analysis for the behavioral sciences*. 2nd edn, (L. Erlbaum Associates, 1988).
51 Sawilowsky, S. S. New Effect Size Rules of Thumb. *Journal of Modern Applied Statistical Methods* **8**, 2 (2009).
52 Koshy Cherian, A. *et al.* Unresponsive Choline Transporter as a Trait Neuromarker and a Causal Mediator of Bottom-Up Attentional Biases. *J Neurosci* **37**, 2947-2959, doi:10.1523/JNEUROSCI.3499-16.2017 (2017).
53 Wong, J. M. *et al.* Benzoyl chloride derivatization with liquid chromatography-mass spectrometry for targeted metabolomics of neurochemicals in biological samples. *Journal of chromatography. A* **1446**, 78-90, doi:10.1016/j.chroma.2016.04.006 (2016).
54 Cardinal, R. N., Parkinson, J. A., Hall, J. & Everitt, B. J. Emotion and motivation: the role of the amygdala, ventral striatum, and prefrontal cortex. *Neurosci Biobehav Rev* **26**, 321-352 (2002).
55 Vertes, R. P. & Hoover, W. B. Projections of the paraventricular and paratenial nuclei of the dorsal midline thalamus in the rat. *J Comp Neurol* **508**, 212-237, doi:10.1002/cne.21679 (2008).
56 Clark, J. J., Collins, A. L., Sanford, C. A. & Phillips, P. E. Dopamine encoding of Pavlovian incentive stimuli diminishes with extended training. *J Neurosci* **33**, 3526-3532, doi:10.1523/JNEUROSCI.5119-12.2013 (2013).

57 Do-Monte, F. H., Quinones-Laracuente, K. & Quirk, G. J. A temporal shift in the circuits mediating retrieval of fear memory. *Nature* **519**, 460-463, doi:10.1038/nature14030 (2015).
58 Giannotti, G., Barry, S. M., Siemsen, B. M., Peters, J. & McGinty, J. F. Divergent Prelimbic Cortical Pathways Interact with BDNF to Regulate Cocaine-seeking. *J Neurosci* **38**, 8956-8966, doi:10.1523/JNEUROSCI.1332-18.2018 (2018).
59 Otis, J. M. *et al.* Prefrontal cortex output circuits guide reward seeking through divergent cue encoding. *Nature* **543**, 103-107, doi:10.1038/nature21376 (2017).
60 Beas, B. S. *et al.* The locus coeruleus drives disinhibition in the midline thalamus via a dopaminergic mechanism. *Nat Neurosci* **21**, 963-973, doi:10.1038/s41593-018-0167-4 (2018).
61 Choi, E. A., Jean-Richard-Dit-Bressel, P., Clifford, C. W. G. & McNally, G. P. Paraventricular thalamus controls behavior during motivational conflict. *J Neurosci*, doi:10.1523/JNEUROSCI.2480-18.2019 (2019).
62 Choi, E. A. & McNally, G. P. Paraventricular Thalamus Balances Danger and Reward. *J Neurosci* **37**, 3018-3029, doi:10.1523/JNEUROSCI.3320-16.2017 (2017).
63 Do-Monte, F. H. & Kirouac, G. J. Boosting of Thalamic D2 Dopaminergic Transmission: A Potential Strategy for Drug-Seeking Attenuation. *eNeuro* **4**, doi:10.1523/ENEURO.0378-17.2017 (2017).
64 Do-Monte, F. H., Minier-Toribio, A., Quinones-Laracuente, K., Medina-Colon, E. M. & Quirk, G. J. Thalamic Regulation of Sucrose Seeking during Unexpected Reward Omission. *Neuron* **94**, 388-400 e384, doi:10.1016/j.neuron.2017.03.036 (2017).
65 Zhu, Y. *et al.* Dynamic salience processing in paraventricular thalamus gates associative learning. *Science* **362**, 423-429, doi:10.1126/science.aat0481 (2018).
66 Zhu, Y., Wienecke, C. F., Nachtrab, G. & Chen, X. A thalamic input to the nucleus accumbens mediates opiate dependence. *Nature* **530**, 219-222, doi:10.1038/nature16954 (2016).
67 Matzeu, A., Cauvi, G., Kerr, T. M., Weiss, F. & Martin-Fardon, R. The paraventricular nucleus of the thalamus is differentially recruited by stimuli conditioned to the availability of cocaine versus palatable food. *Addict Biol* **22**, 70-77, doi:10.1111/adb.12280 (2017).
68 Matzeu, A., Weiss, F. & Martin-Fardon, R. Transient inactivation of the posterior paraventricular nucleus of the thalamus blocks cocaine-seeking behavior. *Neurosci Lett* **608**, 34-39, doi:10.1016/j.neulet.2015.10.016 (2015).

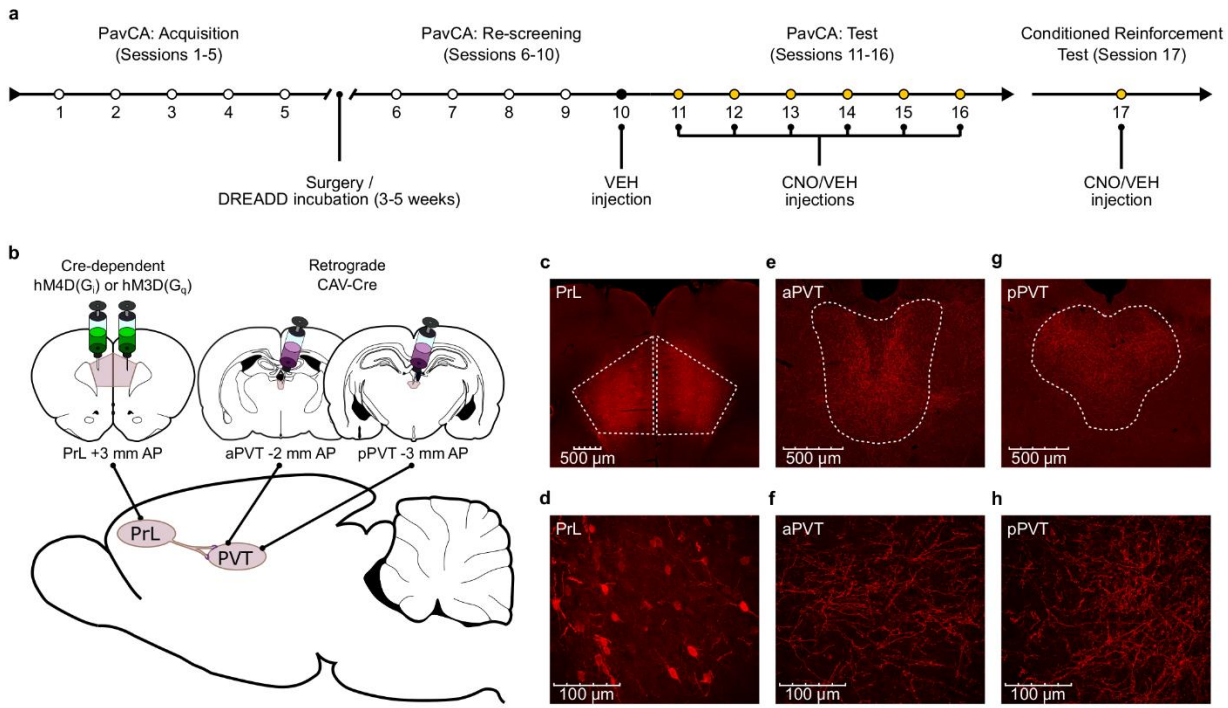

Figure 1. Methods. a) Timeline of the experimental procedures. Rats were trained in a Pavlovian Conditioned Approach (PavCA) paradigm for 5 consecutive days (Acquisition, Sessions 1-5) and phenotyped as sign- (STs) or goal-trackers (GTs). Following acquisition, STs and GTs underwent DREADD surgeries for delivering Gi or Gq DREADDs in neurons of the prelimbic cortex (PrL) projecting to the paraventricular nucleus of the thalamus (PVT). Incubation time for DREADD expression was 3-5 weeks. After Incubation, rats were re-screened for sign- and goal-tracking behavior (Re-screening, Sessions 6-10). All rats received an i.p. VEH injection 25 minutes before session 10 to habituate them to the injection procedure. CNO (3mg/kg) or VEH were then administered i.p. every day during the Test phase (Sessions 11-16), 25 minutes before the start of each session. 24 hours after the last session of PavCA, rats received an additional injection of CNO or VEH 25 minutes before being exposed to a conditioned reinforcement test (CRT, Session 17). **b**) Schematic of the dual-vector strategy used for expressing Gi or Gq DREADDs in the PrL-PVT pathway. **c,d**) Photomicrographs representing mCherry expression in the pyramidal neurons of the PrL projecting to the PVT at (**c**) 4x magnification and (**d**) 40x magnification. **e,f**) Photomicrographs of mCherry expression representing terminal fibers in the anterior PVT coming from the PrL at (**e**) 10x magnification and at (**f**) 40x magnification. **g,h**) Photomicrographs of mCherry expression representing terminal fibers in the posterior PVT coming from the PrL at (**g**) 10x magnification and (**h**) 40x magnification.

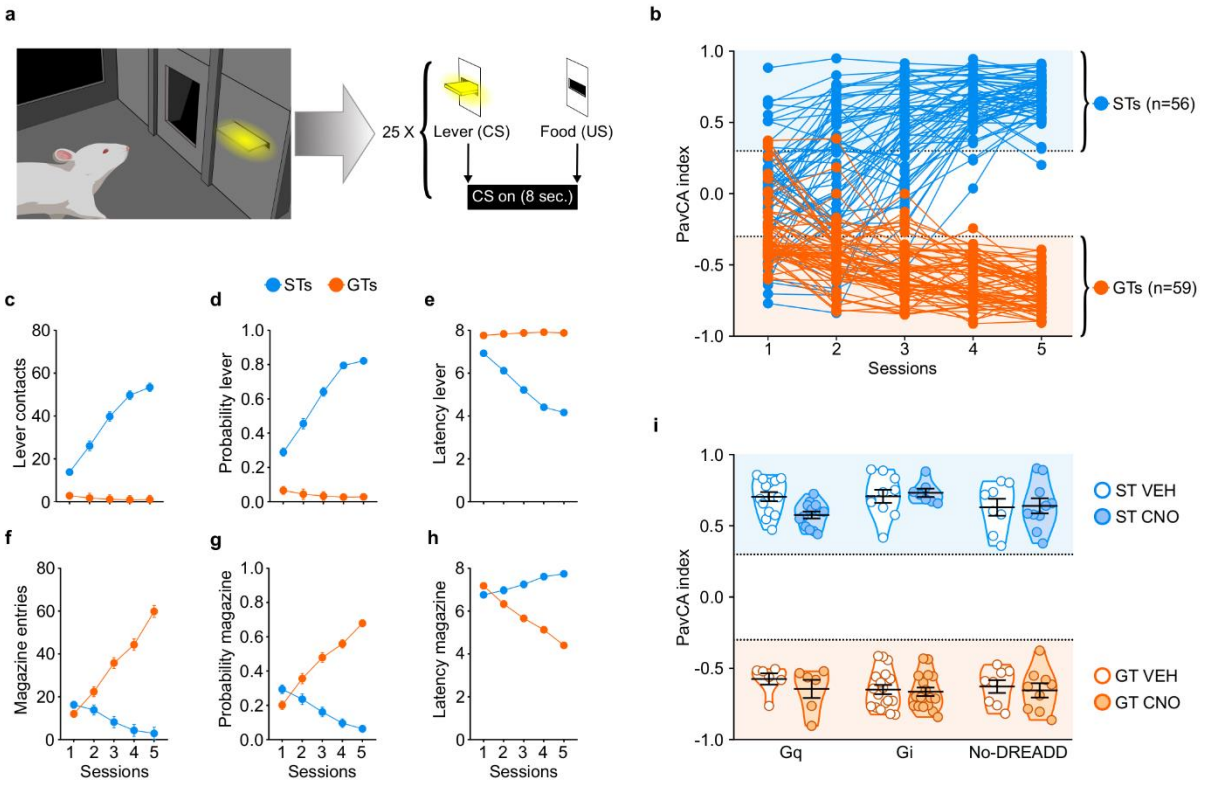

Figure 2. Acquisition of sign- and goal-tracking behaviors across 5 sessions of Pavlovian Conditioned Approach (PavCA) training (i.e. prior to surgery or CNO administration). **a**) Schematic representing the PavCA task. Rats were presented with an illuminated lever (conditioned stimulus, CS) for 8 sec followed by the delivery of a food pellet (unconditioned stimulus, US) immediately upon lever-CS retraction. Each PavCA session consisted of 25 lever-food pairings. **b**) PavCA index scores (composite index of Pavlovian conditioned approach behavior) for individual rats across 5 sessions of Pavlovian conditioning. PavCA index from session 4-5 were averaged to determine the behavioral phenotype. Rats with a PavCA score <-0.3 were classified as goal-trackers (GTs, n=59), rats with a PavCA score >+0.3 were classified as sign-trackers (STs, n=56). **c-e**) Acquisition of lever-directed behaviors (sign-tracking) during PavCA training. Mean ± SEM for (**c**) number of lever contacts, (**d**) probability to contact the lever, and (**e**) latency to contact the lever. **f-h**) Acquisition of magazine-directed behaviors (goal-tracking) during PavCA training. Mean ± SEM for (**f**) number of magazine entries, (**g**) probability to enter the magazine, and (**h**) latency to enter the magazine. **i**) Data are expressed as individual data points with mean ± SEM plotted on violin plots for PavCA index. Rats with similar PavCA index scores were counterbalanced across different GPCR (Gi, Gq or no-DREADD) and different treatment (CNO, VEH) groups. Baseline differences in PavCA index between

experimental groups were assessed by using a 3-way ANOVA with Phenotype (GT, ST), DREADD (Gi, Gq and no-DREADD) and Treatment (CNO, VEH) as independent variables and PavCA index as the dependent variable. There was a significant effect of phenotype ($p < 0.001$), but no significant differences between experimental groups. Sample size: GT-Gi=32, GT-Gq=12, ST-Gi=14, ST-Gq=25, GT-no DREADD=15, ST-no DREADD=17.

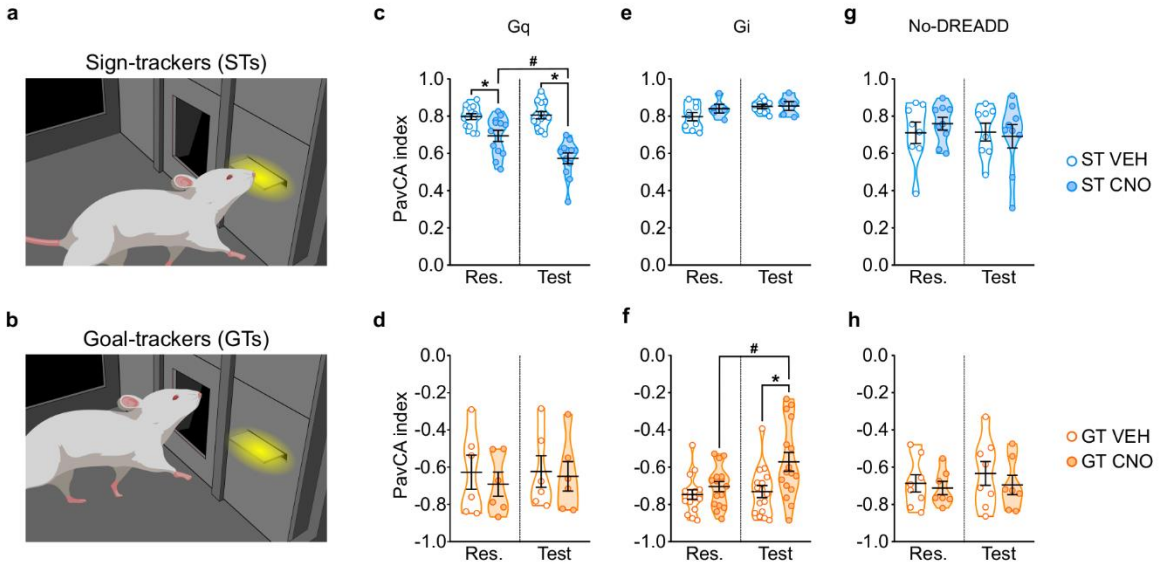

Figure 3. Chemogenetic stimulation of the PrL-PVT pathway decreases the incentive value of a food cue in sign-trackers, while chemogenetic inhibition of the PrL-PVT pathway increases the incentive value of a food cue in goal-trackers. a,b) Drawing representative of the conditioned response that characterizes (**a**) sign-trackers and (**b**) and goal-trackers. **c-h**) Data are expressed as individual data points with mean ± SEM plotted on violin plots for PavCA index during Rescreening (Res., average of PCA Sessions 6-10) and Test (average of PCA Sessions 11-16) periods. **c,d**) Chemogenetic stimulation (Gq) of the PrL-PVT circuit decreases the PavCA index in (**c**) sign-trackers, but has no effect in (**d**) goal-trackers. There was a significant treatment x session interaction in sign-trackers ($p<0.01$; *$p<0.001$, CNO vs. VEH; #$p<0.001$, CNO Test vs. CNO Res.). **e,f**) Chemogenetic inhibition of the PrL-PVT circuit has no effect on (**e**) sign-trackers, but increases the PavCA index in (**f**) goal-trackers (*$p<0.012$, CNO vs. VEH; #$p<0.002$ CNO Test vs. CNO Res.). **g,h**) Effects of CNO administration on the PavCA index in non-DREADD expressing (**g**) STs and GTs (**h**). When DREADD receptors were not expressed in the brain, CNO had no effect on the PavCA index in either sign-trackers nor goal-trackers. Sample size: GT-Gi=32, GT-Gq=12, ST-Gi=14, ST-Gq=25, GT-no DREADD=15, ST-no DREADD=17.

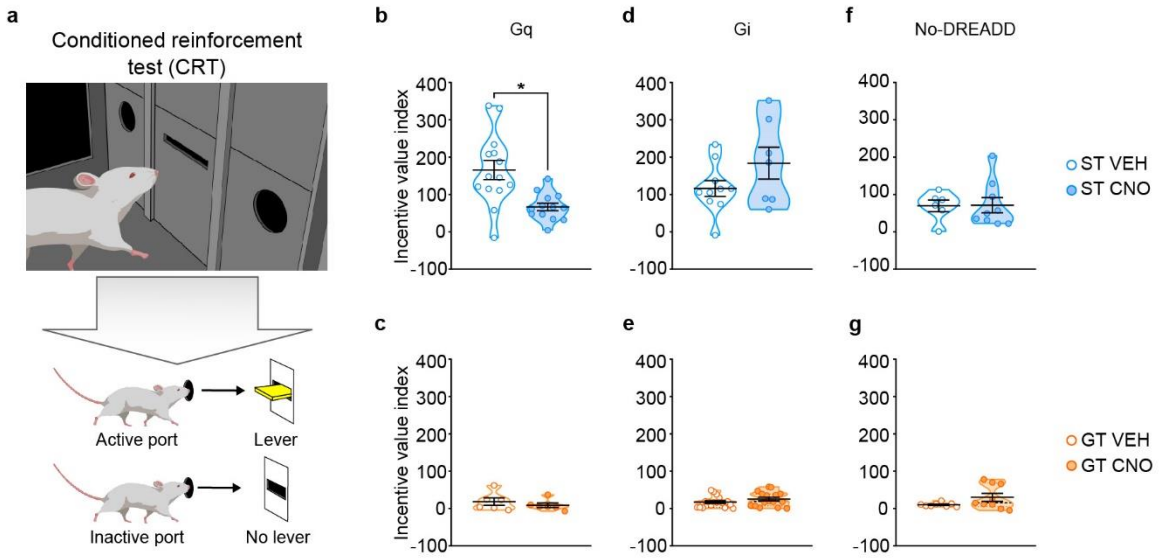

Figure 4. Chemogenetic stimulation of the PrL-PVT pathway decreases the conditioned reinforcing properties of a reward-paired cue in sign-trackers. **a**) Schematic representing the conditioned reinforcement test. Data are expressed as individual data points with mean ± SEM plotted on violin plots for Incentive value index (active nosepokes + lever presses - inactive nosepokes). **b,c**) Relative to VEH controls, administration of CNO (3 mg/kp, i.p.) significantly decreased the incentive value of the reward cue for (**b**) ST-Gq (*p<0.05), but not (**c**) GT-Gq rats. **d,e**) CNO-induced inhibition of the PrL-PVT circuit did not affect the conditioned reinforcing properties of the reward cue in (**d**) ST-Gi or (**e**) GT-Gi rats. **f,g**) CNO administration did not affect the conditioned reinforcing properties of the reward cue in non-DREADD expressing (**f**) STs or (**g**) GTs. Sample size: GT-Gi=32, GT-Gq=12, ST-Gi=14, ST-Gq=25, GT-no DREADD=15, ST-no DREADD=17.

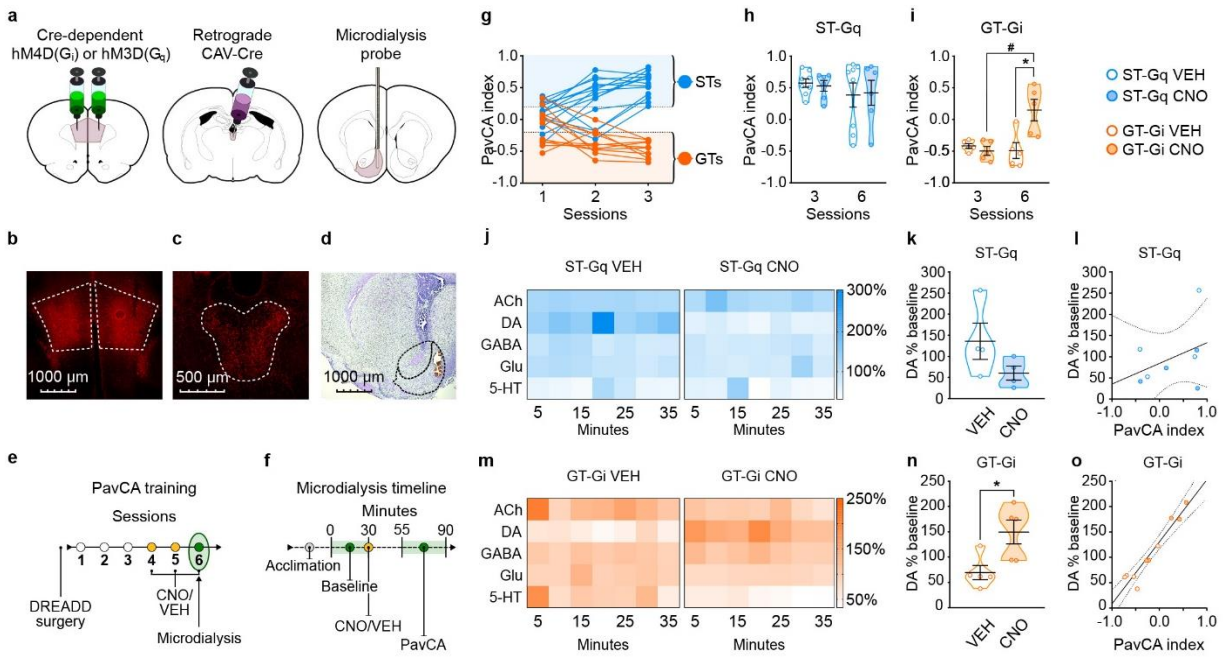

Figure 5. Inhibition of the PrL-PVT circuit early in Pavlovian training increases the propensity to sign-track and increases extracellular levels of dopamine in the nucleus accumbens shell (NAcS) of GT rats. **a**) Schematic of the cannulation surgery and the dual-vector strategy used for expressing Gi DREADDs in the PrL-PVT pathway of GTs, or Gq DREADDs in the PrL-PVT pathway of STs. **b-d**) Representative images of coronal brain sections showing mCherry expression in the (**b**) PrL (5x magnification) and (**c**) PVT (10x magnification), and (**d**) placement of the microdialysis probe in the NAcS (5x magnification). **e**) Experimental timeline. After surgery and DREADD incubation, rats were trained in a PavCA task for 3 sessions (1-3) and classified as STs or GTs. Rats then received CNO (3mg/kg, i.p.) or vehicle (VEH) 25 minutes before being trained for 3 additional sessions (4-6) of PavCA. **f**) Microdialysis timeline. Before the start of Session 6 of PavCA training, microdialysis probes were inserted into the guide cannula and rats were left undisturbed for 2 hours before starting sample collection (acclimation period). After acclimation, 6 baseline dialysates were collected over 30 minutes before injecting rats with either CNO or vehicle (VEH). Session 6 of PavCA training started 25 minutes after CNO/VEH injections, and 7 fractions of dialysate were collected during the session. **g**) Individual PavCA index scores during the first 3 sessions of Pavlovian conditioning. Rats with a PavCA index <-0.2 were classified as GTs (n=10), rats with a PavCA index >+0.2 were classified as STs (n=13). **h,i**) Data are expressed as mean ± SEM for PavCA index. (**h**) CNO during session 6 of training did not affect the PavCA index in ST-Gq rats. (**i**) CNO during session 6 of training significantly increased the PavCA index in GT-Gi rats

(*p=0.016 vs. VEH; #p=0.009 vs. session 3). **j,m**) Heatmaps showing the relative percent (%) change from baseline of acetylcholine (ACh), dopamine (DA), GABA, glutamate (Glu) and serotonin (5-HT) in the NAc shell during Session 6 of PavCA training in (**j**) ST-Gq rats (blue) and (**m**) GT-Gi rats (orange). **k,n**) Mean ± SEM levels of DA % change during Session 6 of Pavlovian conditioning in (**k**) ST-Gq and (**n**) GT-Gi rats. There was a significant effect of CNO for GT-Gi rats (*p= 0.008). **l,o**) Bivariate scatterplots illustrating the relationship between DA % change from baseline and PavCA index during session 6 of PavCA training. There was not a significant correlation in (**l**) ST-Gq rats, but there was a significant positive correlation between percent change in DA and PavCA index in (**o**) GT-Gi rats (r^2 =0.92; p<0.001). Sample size: Behavior, GT-Gi=10; ST-Gq=13; microdialysis data, GT-Gi=10; ST-Gq=8.

THE PARAVENTRICULAR THALAMUS IS A CRITICAL MEDIATOR OF TOP-DOWN CONTROL OF CUE-MOTIVATED BEHAVIOR

Supplementary Methods and Materials

Subjects. Rats from Experiment 1 and 2 were 7-9 weeks old at the time of arrival. Rats were housed in a climate-controlled room (22±2 °C) with a 12-hour dark-light cycle (lights on at 06:00 AM or 07:00 AM depending on daylight savings time) and allowed to acclimate to the colony room for at least 1 week prior to handling. All rats had *ad-libitum* access to food and water for the duration of the experiments. Rats from Experiment 1 were paired-housed for the duration of the experiments. Rats from Experiment 2 were single-housed after cannula implantation to avoiding damage to the implants. Behavioral testing took place during the light cycle between 11:00 AM and 5:00 PM. All procedures followed The Guide for the Care and Use of Laboratory Animals: Eighth Edition (2011, National Academy of Sciences) and were approved by the University of Michigan Institutional Animal Care and Use Committee.

Pavlovian conditioned approach (PavCA)

Apparatus. PavCA training occurred inside Med Associates chambers (St. Albans, VT, USA; 30.5 × 24.1 × 21 cm) located in sound-attenuating cabinets with a ventilation fan to mask background noise. Each chamber contained of a food magazine located in the center of one wall located 3 cm above the grid floor, connected to an automatic pellet dispenser. A retractable backlit metal lever was located either to the left or right of the food magazine, 6 cm above the grid floor. A house light was located on the wall opposite to the food magazine and lever, 1 cm from the top of the chamber. Magazine entries were recorded upon break of a photo-beam located inside the magazine and a lever contact was registered upon deflection, which required a minimum of a 10-g force.

PavCA procedures. PavCA procedures were the same as those described previously[1]. For two days before the start of behavioral procedures, rats were handled by the experimenters and given ~25 banana-flavored food pellets (45 mg dustless pellets, Bio-Serv, Flemington, NJ, USA) in order to familiarize them with the food reward that served as the US during PavCA training. After this period, rats underwent two pre-training

sessions, consisting of 25 trials in which a food pellet was delivered into the food magazine on a variable time (VT) 30-s schedule (range 0-60 s). During pre-training, head entries into the food magazine were recorded to ensure that rats retrieved all of the food pellets. Each session lasted approximatively 12.5 minutes. After pre-training, rats underwent one daily session of PavCA training for 5 consecutive days. Each PavCA training session consisted of 25 trials under a VT-90 s schedule (range 30-150 s), during which the presentation of an illuminated lever-CS for 8 seconds was followed by the delivery of a banana-flavored food pellet into the food magazine. The start of PavCA training was signaled by illumination of the house light and lasted an average of 40 minutes. For each PavCA session, the number of lever-CS contacts and head entries into the food magazine, the probability of contacting the lever-CS or entering the food magazine, and the latency to contact the lever-CS or to enter the food magazine during each trial were recorded. These measures were used to calculate a PavCA index as previously described[1]. Briefly, the PavCA index is a composite score that captures the propensity to approach the lever-CS relative to the food magazine. It is calculated by averaging 3 distinct measures: 1) response bias [(total lever-CS contacts − total food magazine entries) / (total lever-CS contacts + total food magazine entries)], 2) probability difference [$Prob_{(lever)} - Prob_{(food\ magazine)}$] and, 3) latency difference [−(latency to contact the lever-CS – latency to enter the food magazine)/8]. The PavCA index ranges from +1 to -1. A score of -1 indicates an extreme GT whose conditioned responses are always directed toward the food magazine, while a score of +1 indicates an extreme ST whose conditioned responses are always directed toward the lever-CS. For experiment 1, rats with an average PavCA index ≥ +0.30 during session 4 and 5 were classified as STs, while rats with an index ≤ -0.30 were classified as GTs.

Dual-vector DREADD surgery. The anesthetic plane was induced with 5% isoflurane (Isothesia - Butler-Schein, Columbus, OH) and maintained throughout the procedure with 2% isoflurane. Prior to surgeries, rats received an injection of carprofen (5.0 mg/kg, s.c.) for analgesia, and the scalp was shaved and sterilized with Betadine solution (Betadine, Stamford, CT) and 70% alcohol pads. Rats were then fitted into a stereotaxic frame (David Kopf instruments, Tujunga, CA or Stoelting, Wood Dale, IL), a small incision was made on the scalp to expose the skull, and small burr holes were drilled

above the regions of interest. A 31-gauge stainless steel injector (Plastics One, Roanoke, VA) connected to a 5-□L Hamilton microsyringe (Hamilton Company, Reno, NV) was inserted bilaterally into the PrL (+3.0 mm AP; ± 1.0 mm ML; -4 mm DV, relative to bregma) for the delivery of 1 □L of either Gq or Gi Cre-dependent DREADD viruses at a rate of 200 nL per minute over a 5-min period using a micro pump (Elite 11, Harvard Apparatus, Holliston, MA). CAV2-Cre was injected at a 10° angle into the aPVT (-2.0 mm AP; -1 mm ML; -5.4 mm DV, relative to bregma) and pPVT (-3.0 mm AP; -1 mm ML; -5.5 mm DV, relative to Bregma) using a 1 µL Neuros syringe (Hamilton Company, Reno, NV) mounted on a Kopf Model 5000 Microinjection Unit (David Kopf Instruments, Tujunga, CA, USA), at a rate of 50 nL per minute for 2 minutes (100 nL total volume). Following delivery, needles were left in place for an additional 5 minutes to allow diffusion. After surgery, rats were left undisturbed for 3-5 weeks, a time period we found optimal for the expression of DREADD constructs (Fig. S1).

Perfusion and tissue processing. Approximately one week after completing the behavioral experiments, rats were anesthetized with ketamine (90 mg/kg i.p.) and xylazine (10 mg/kg i.p.) and transcardially perfused with 0.9% saline followed by 4% formaldehyde (pH= 7.4) for fixation. Brains were extracted, post-fixed in 4% formaldehyde for 24 hours at 4°C and immersed in increasing concentrations of sucrose solutions every 24 h (10%, 20% then 30% sucrose in 0.1M PBs, pH= 7.4) at 4°C over the course of 3 days. Brains were then encased in Tissue-Plus O.C.T. (Fisher HealthCare, Houston, TX), frozen using dry ice and subsequently sectioned in the coronal plane (40 □m) using a cryostat (Leica Biosystems Inc, Buffalo Grove, IL). For experiment 1, brain slices from the PrL (ranging from +5.00 to +2.5 mm AP, relative to Bregma) and PVT (ranging from -1.00 to -4.00 mm AP, relative to Bregma) were placed into well plates containing cryoprotectant and stored at -20°C in until further processing.

Immunohistochemistry. The accuracy of DREADD expression in the PrL and PVT was assessed using immunohistochemical staining methods to visualize the mCherry protein in DREADD-expressing neurons. Free-floating coronal sections from the PrL and PVT were first rinsed 3 times in 0.1M PBS (pH= 7.4). Endogenous peroxidase activity was blocked by incubating sections in 1% H_2O_2 for 10 minutes, followed by 3 additional rinses. To prevent non-specific binding of the secondary antibody, sections

were incubated in 0.1M PBS containing 0.4% Triton X-100 (TX) and 2.5% Normal Donkey Serum (NDS) (Jackson ImmunoResearch Laboratories, Inc., West Grove, PA). Sections were then incubated overnight at room temperature in primary antibody (rabbit anti-mCherry, Abcam, Cambridge, UK, diluted 1: 30,000) in 0.1M PBS + 0.4% TX + 1% NDS. On the following day, sections were rinsed again before being incubated for 1h in a biotinylated donkey anti-rabbit secondary antibody (Jackson Immunoresearch, West Grove, PA, diluted 1: 500) in 0.1M PBS + 0.4% TX + 1% NDS. Peroxidase staining was obtained with a standard avidin-biotin procedure using the Vectastain Elite ABC Kit (Vector Laboratories, Inc., Burlingame, CA diluted 1: 1000 for A and B). Chromogenic reaction occurred by incubating sections in a 0.1M PBS solution containing 0.02% 3,3'-diaminobenzidine tetrahydrochloride (DAB) and 0.012% H_2O_2. Sections were rinsed and stored at 4°C until mounted, air dried and cover-slipped with Permount (Thermo-Fisher Scientific, Waltham, MA). Bright-field images containing the PrL, aPVT and pPVT were captured using a Leica DM1000 light microscope (Leica-Microsystems, Wetzlar, GER) and were analyzed by two experimenters blind to the experimental groups.

Two or three experimenters who were blind to group assignments scored each image according to both the intensity and location of DREADD expression in the areas of interest (Fig. S1). A score of 0 was assigned to subjects that had no DREADD expression or off target DREADD expression (e.g. expression outside target boundaries) in either the PrL or the aPVT and pPVT; a score of 1 was assigned to subjects that had “adequate” intensity of DREADD expression in both the PrL and PVT; a score of 2 was assigned to subjects that had “adequate” intensity of DREADD expression in one region (i.e. PrL or PVT) and “strong” intensity in the other; and a score of 3 was assigned to subjects that had “strong” intensity of DREADD expression in both the PrL and PVT. Only those rats who had two experimenters score them as 1 or greater were included in the final dataset. Rats that had a score of 0 (n= 65) were excluded.

To generate representative photomicrographs (Fig. 1), DREADD expression in the PrL and PVT was assessed in a subset of brains using immunofluorescence to visualize mCherry in DREADD-expressing neurons. Sections were incubated overnight at room temperature in primary antibody (rabbit anti-mCherry, Abcam, Cambridge, UK, diluted 1:

500) in 0.1M PBS + 0.4% TX + 2.5% NDS. On the following day, sections were rinsed and incubated for 2h in a biotinylated donkey anti-rabbit secondary antibody (Jackson Immunoresearch, West Grove, PA, diluted 1: 500) in 0.1M PBS + 0.4% TX + 2.5% NDS. Sections were rinsed again and then incubated for 1h in Alexa Fluor™ 594-conjugated streptavidin (Thermo Fisher Scientific, Waltham, MA, diluted 1:1000) in 0.1M PBS + 0.4% TX. Sections were then mounted onto slides and cover-slipped with ProLong™ Gold Antifade Mountant (Thermo Fisher Scientific, Waltham, MA). Fluorescent pictures containing the PrL, aPVT and pPVT were captured using a Zeiss AxioImager M2 motorized fluorescent microscope with Apotome structured illumination (Carl Zeiss, Sweden).

Experiment 1 Detailed Methods

PavCA rescreening vs. PavCA test. To test the effects of either stimulation (i.e. Gq-expressing rats) or inhibition (i.e. Gi-expressing rats) of the PrL-PVT pathway on the expression of a Pavlovian conditioned approach response, we compared the average PavCA index during PavCA rescreening (sessions 6-10, prior to treatment) with the average PavCA index during test (sessions 11-16, concurrent with treatment). These analyses were conducted independently for each phenotype and GPCR (i.e. Gq, Gi or no-DREADD). For all analyses, session (rescreening vs. test) was used as the within-subject independent variable and treatment (CNO, VEH) as the between-subject independent variable. PavCA index is presented as the primary dependent variable in the main text, but analyses for other dependent variables are included in Supplemental Results.

Conditioned reinforcement test (CRT). The day after the completion of PavCA training, rats were exposed to a conditioned reinforcement test (CRT). For CRT, conditioning chambers were reconfigured such that the food magazine was removed, and the retractable lever was placed in the center of the wall flanked by a nose-port on either side. Nose pokes into one port (active port), resulted in the presentation of the illuminated lever for 2s on a fixed-ratio 1 (FR1) schedule; nose pokes into the opposite port (inactive port) had no consequence. To minimize side bias, the active port was always placed opposite the side the lever-CS was located during PavCA sessions. The

conditioned reinforcement test lasted 40 min, and the following behaviors were recorded: number of lever contacts, number of nose pokes into the active port (active nose pokes) and number of nose pokes into the inactive port (inactive nose pokes). A composite score, the incentive value index[2], was then used to capture all of the behavioral measures obtained during the conditioned reinforcement test: (active nose pokes + lever presses – inactive nose pokes).

Statistical analyses. Acquisition of sign- and goal-tracking behavior during sessions 1-5 of PavCA training was analyzed using the following dependent variables: number of lever contacts, number of magazine entries during the CS period, probability to contact the lever, probability to enter the magazine during the CS period, latency to contact the lever and latency to enter the magazine during the CS period. To assess differences in the acquisition of sign- and goal-tracking behaviors during PavCA training a linear mixed-effects model (LMM) with a Restricted Maximum Likelihood (REML) estimation method was used. Session was used as the repeated variable and GPCR (three levels: Gq, Gi and No-DREADD), phenotype (two levels: GT, ST) and treatment (two levels: CNO, VEH) as between-subject variables. Before choosing the final model, all covariance structures were explored for each one of the dependent variables and the best fitting model was chosen by selecting the lowest Akaike Information criterion (AIC)[3, 4]. To explore the existence of baseline differences between different experimental groups after PavCA training (and prior to surgery), the average PavCA index from session 4 and 5 was analyzed by using a 3-way ANOVA with phenotype (GT, ST), GPCR (Gq, Gi and No-DREADD) and treatment (CNO, VEH) as independent variables. It should be noted that comparisons between phenotypes and treatment groups were only made for the acquisition phase of PavCA behavior, as it is important to demonstrate that the phenotypes differ in their conditioned response and that the classification and assignment to (Gq, Gi, No-DREADD) and treatment (CNO, VEH) group was balanced within phenotype according to these measures.

To test the effects of either stimulation (i.e. Gq-expressing rats) or inhibition (i.e. Gi-expressing rats) of the PrL-PVT pathway on the expression of a Pavlovian conditioned approach response, we compared the average PavCA index during PavCA rescreening (sessions 6-10, prior to treatment) with the average PavCA index during test (sessions

11-16, concurrent with treatment). Thus, the PavCA index from sessions 6-10 of PavCA rescreening and from the PavCA test (sessions 11-16) were averaged and compared for each GPCR and Phenotype using a LMM with REML as the estimation method. Session (two levels: rescreening, test) was used as the repeated measure and treatment (two levels: CNO, VEH) as the between-subject variable.

To analyze the effect of CNO administration on the behaviors expressed during the CRT test, nose pokes, lever contacts and incentive value index during CRT were analyzed separately for each GPCR and Phenotype. Nose pokes were analyzed using a two-way ANOVA with nose port (two levels: active, inactive) and treatment (two levels: CNO, VEH) as independent variables. Differences between CNO- and VEH-treated animals for lever contacts and the incentive value index were analyzed using an unpaired t-test.

For LMM analyses, normality was checked with a Shapiro-Wilk test. If normality was violated, the presence of outliers and influential data points was explored by using boxplots, Cook's distance and Covariance ratio[5]. Outliers were excluded from the statistical analysis until normality was met. Importantly, however, the results of the statistical analyses were the same with or without the outliers. Graphical representations include only those data without outliers. All statistical analyses were performed using IBM SPSS Statistics 24 (IBM, Armonk, NY, USA). Alpha was set at 0.05. When significant main effects or interactions were detected, Bonferroni post-hoc comparisons were performed. Effects sizes for pairwise comparisons were calculated using Cohen's d[6,7], as previously reported[2].

Experiment 2 Detailed Methods

Drugs. All chemicals, drugs, and reagents were purchased from Sigma-Aldrich unless otherwise noted. HPLC grade water was purchased from Thermo-Fisher Scientific (Waltham, MA) and HPLC grade acetonitrile was purchased from VWR (Radnor, PA).

Microdialysis. Microdialysis collection occurred on session 6 of PavCA training. Rats were temporarily anesthetized with 5% isoflurane, the wire stylets were removed from the guide cannula and a microdialysis probe (CMA 12 Elite probe, 2 mm membrane length, 20 kDA molecular cut-off, Harvard Apparatus, Holliston, MA) was inserted to

reach the NAc Shell. Rats were then placed inside conditioning chambers adapted for microdialysis. These chambers were different from the ones used during the previous PavCa training sessions, but the lever-CS and the food magazine were located in the same side of the chamber. After probe insertion, rats were left undisturbed in the conditioning chamber for 120 minutes while the probes were continuously perfused at a rate of 1.0 µl/min with artificial cerebrospinal fluid (aCSF, pH 7.4) containing, in mM: 145.00 NaCl, 2.68 KCl, 1.10 MgSO4, 1.22 CaCl2, 0.50 NaH2PO4, 1.55 Na2HPO4. Immediately before starting perfusion aCSF was added with 0.25 mM ascorbic acid to prevent dopamine oxidation. Dialysate samples (5 □l) were collected every 5 minutes, beginning 120 minutes after inserting the probes. Baseline samples were collected for 30 minutes (6 fractions); after this time rats were injected with CNO/VEH and samples were collected for additional 25 minutes (pre-PavCA samples, 5 fractions). PavCA training started 25 minutes after CNO/VEH injections. Samples were collected during the PavCA session across a period of 35 minutes (PavCA samples, 7 fractions). After collection, samples were derivatized as described below and stored at -80°C until they were analyzed by high-performance liquid chromatography-tandem mass spectrometry (HPLC-MS).

Benzoyl chloride derivatization. Benzoyl chloride derivatization of dialysates and internal standards was performed using a modified version of the methods described in[8]. Calibration curves were generated using standards at 0, 0.1, 0.5, 1, 5, 10, and 20 nM for DA. Internal standards (IS) stock solutions were derivatized by adding 100 mM sodium carbonate monohydrate buffer, followed by 2% $^{13}C_6$ benzoyl chloride in acetonitrile with 0.1% formic acid. The IS stock was then diluted 100-fold in a 50:50 acetonitrile/H_2O solution containing 1% sulfuric acid. Calibration standards and dialysate samples were derivatized by adding them with 100 mM sodium carbonate buffer, 2% benzoyl chloride (in acetonitrile), and an internal standard in a 2:1:1:1 ratio.

HPLC-MS. A Thermo Finnigan Surveyor Plus HPLC system was used for analyzing microdialysis samples. Neurochemical separation was achieved with a Phenomenex (Torrance, CA) Kinetex biphenyl LC column (50 × 2.1 mm, 1.7 µm particle size, 100 Å pore size). Mobile phase A was 10 mM ammonium formate and 0.15% (v/v) formic acid in HPLC water. Mobile phase B was acetonitrile. The mobile phase gradient for all of the

analytes was: initial, 0% B; 0.1 min, 10% B; 0.12 min, 10% B; 2.3 min, 20% B; 3.7 min, 50% B; 4.0 min, 80% B; 4.5 min, 100% B; 5.0 min 100% B; 6.5 min, 0% B. The flow rate was 200 µL/min, and the sample injection volume was 7 µL. The autosampler and column were maintained at ambient temperature throughout the analysis. A Thermo Finnigan TSQ Quantum Ultra triple quadrupole mass spectrometer operating in positive mode was used for detection. Electrospray ionization (ESI) voltage was 3.5 kV, and heated ESI probe (HESI-I) was set at 300°C. Capillary temperature was 350°C, and sheath gas, aux gas, and ion sweep gas were maintained at 25, 15, and 0 arb, respectively. The intercycle delay was 200 ms. Automated peak integration was performed using Thermo XCalibur QuanBrowser version 2.1. All peaks were visually inspected to ensure proper integration. Calibration curves were constructed based on peak area ratio ($P_{analyte}/P_{IS}$) versus concentrations by linear regression.

Immunohistochemistry and histology. Upon completion of experimental procedures, brain tissue was processed for the assessment of DREADD expression as described above. To identify the placement of the microdialysis probes, brain slices containing the NAc shell (bregma 1.70-1.00 mm AP) were mounted onto glass slides, stained using Cresyl-violet (Sigma-Aldrich, St. Louis, MO) and cover-slipped with a toluene-based solution (Permount, Fisher Scientific, Fair Lawns, NJ). Verification of probe placement was done using a Leica DM1000 light microscope (Buffalo Grove, IL) by two experimenters blind to experimental groups. Only rats with probe placements within the NAc shell were included in the statistical analyses.

Statistical analyses. Acquisition of sign- and goal-tracking behavior during sessions 1-3 of PavCA training was analyzed using the same dependent variables described above: number of lever contacts, number of magazine entries during the CS period, probability to contact the lever, probability to enter the magazine during the CS period, latency to contact the lever and latency to enter the magazine during the CS period. To assess differences in the acquisition of sign- and goal-tracking behaviors during PavCA training a LMM with a REML estimation method was used. Session was used as the repeated variable and group (two levels: GT-Gi, ST-Gq) and treatment (two levels: CNO, VEH) as between-subject variables. The best fitting model was chosen by selecting the lowest AIC. To explore the existence of baseline differences between

different experimental groups after PavCA training, the PavCA index from session 3 was analyzed by using a 2-way ANOVA with group (GT-Gi, ST-Gq), and treatment (CNO, VEH) as independent variables. For the same reasons as those described above for Experiment 1, this is the only analysis for which the two groups were directly compared. To analyze the effects of CNO administration within each group, the PavCA index expressed after the initial acquisition (Session 3) was compared with the PavCA index expressed after 3 days of treatment (Session 6). Session (3 vs. 6) was used as the repeated measure and treatment (CNO, VEH) as the between-subject variable within each group. Data were analyzed using a LMM with REML as estimation method. Microdialysis data were also analyzed separately for ST-Gq and GT-Gi rats. The following neurotransmitters were analyzed: gamma-Aminobutyric acid (GABA), glutamate (Glu), dopamine (DA), serotonin (5-HT) and acetylcholine (ACh). For all neurotransmitters analyzed, differences between treatment groups in the baseline levels were analyzed using an unpaired sample t-test. Levels of neurotransmitters obtained during the subsequent block of collection (pre-PavCA and PavCA) were expressed in terms of percentage (%) change from baseline. Differences in the % change from baseline for each neurotransmitter were analyzed by using a LMM with a REML estimation method. Time (Pre-PavCA, PavCA) was used as a repeated measure and treatment (CNO, VEH) as a between-subjects independent variable. Differences in the averaged % change from baseline during PavCA training were analyzed using a t-test. The relationship between DA and PavCA index during session 6 of PavCA training was examined using a linear regression with % change of DA as the predictor and PavCA index as dependent variable. A one-way ANOVA with PavCA index as dependent variable and treatment (VEH, CNO) as dependent variable and the predictor (% DA) as a covariate was used to assess if the relationship between DA and PavCA index changed as a function of treatment. All statistical analyses were performed using IBM SPSS Statistics 24 (IBM, Armonk, NY, USA). Alpha was set at 0.05. When significant main effects or interactions were detected, Bonferroni post-hoc comparisons were performed. Effects sizes were calculated using Cohen’s d. For group comparison, data are illustrated plotting individual data points with mean and SEM on a violin plot showing the probability of the distribution of the dependent variable for each value. All graphical

representations of the data were made with Prism 8 (Graphpad Software, San Diego, CA). Violin plots and individual data points with mean ± SEM were overlaid using Inkscape 0.92.

Supplemental Results

Analysis of nosepokes and lever contacts during CRT. The effect of chemogenetic manipulation of the PrL-PVT pathway on nosepokes into the active and inactive port and contacts with the lever-CS during CRT are reported in Figure S2. For ST-Gq, there was a significant effect of treatment ($F_{1,36}$ =19.021, p<0.001), port ($F_{1,36}$ =30.501, p<0.001) and a significant treatment x port interaction ($F_{1,36}$=7.024, p<0.05) for nosepoke responding. Post-hoc analysis revealed that stimulation of the PrL-PVT in STs decreased the number of nose pokes into the active port compared to VEH-treated subjects (p<0.001, Cohen's d=1.55), and abolished the discrimination between pokes into the active and inactive ports (p < 0.001, Cohen's d=1.63). Stimulation of the PrL-PVT pathway in STs also reduced the number of lever contacts ($t_{18.142}$ =-3.615, p<0.05, Cohen's d=1.47, Fig. S3g). Together, these data support the notion that "turning on" top down PrL-PVT control in STs attenuates the incentive motivational value and conditioned reinforcing properties of the lever-cue. Furthermore, consistent with the data presented in the main text, there was not a significant effect of inhibiting the PrL-PVT pathway on any measures of conditioned reinforcement for either STs or GTs, nor was there an effect of stimulating PrL-PVT in GTs, nor CNO administration in non-DREADD controls (Fig. S3).

References

1 Meyer, P.J., et al., *Quantifying individual variation in the propensity to attribute incentive salience to reward cues.* PLoS One, 2012. **7**(6): p. e38987.

2 Hughson, A.R., et al., *Incentive salience attribution, "sensation-seeking" and "novelty-seeking" are independent traits in a large sample of male and female heterogeneous stock rats.* Sci Rep, 2019. **9**(1): p. 2351.

3 Duricki, D.A., S. Soleman, and L.D. Moon, *Analysis of longitudinal data from animals with missing values using SPSS.* Nat Protoc, 2016. **11**(6): p. 1112-29.

4 Verbeke, G. and G. Molenberghs, *Linear mixed models for longitudinal data*. Springer series in statistics. 2009, New York: Springer. xxii, 568 p.

5 West, B.T., et al., *Linear mixed models : a practical guide using statistical software*. Second edition. ed. 2015, Boca Raton: CRC Press, Taylor & Francis Group. xxv, 414 pages.

6 Cohen, J., *Statistical power analysis for the behavioral sciences*. 2nd ed. 1988, Hillsdale, N.J.: L. Erlbaum Associates. xxi, 567 p.

7 Sawilowsky, S.S., *New Effect Size Rules of Thumb.* Journal of Modern Applied Statistical Methods, 2009. **8**(2): p. 2.

8 Song, P., et al., *In vivo neurochemical monitoring using benzoyl chloride derivatization and liquid chromatography-mass spectrometry.* Anal Chem, 2012. **84**(1): p. 412-9.

Table S1. Acquisition of Pavlovian conditioned approach during PavCA Sessions 1-5: lever-directed behaviors.

	Lever-directed behaviors (Sign-tracking)								
	ST-Gq								
	Lever contacts			Probability lever			Latency lever		
	DF	F	p	DF	F	p	DF	F	p
Treatment	1,22.854	2.347	0.139	1,25.783	4.368	**<0.05**	1,24.682	3.673	0.067
Session	4,32.488	29.080	**<0.01**	4,56.630	53.553	**<0.01**	4,59.141	49.482	**<0.01**
*Treatment*session*	4,32.488	2.516	0.061	4,56.630	3.734	**<0.01**	4,59.141	3.875	**<0.01**
	GT-Gq								
	Lever contacts			Probability lever			Latency lever		
	DF	F	p	DF	F	p	DF	F	p
Treatment	1,10.000	0.254	0.625	1,10.000	0.023	0.883	1,10.000	0.058	0.815
Session	4,10.000	3.717	**<0.05**	4,10.000	1.551	0.261	4,10.000	3.193	0.062
*Treatment*session*	4,10.000	1.597	0.250	4,10.000	1.356	0.316	4,10.000	2.296	0.131
	ST-Gi								
	Lever contacts			Probability lever			Latency lever		
	DF	F	p	DF	F	p	DF	F	p
Treatment	1,15.551	0.001	0.982	1,12.941	0.113	0.742	1,12.879	0.000	0.989
Session	4,46.408	8.800	**<0.01**	4,26.870	8.342	**<0.01**	4,33.398	16.017	**<0.01**
*Treatment*session*	4,46.408	0.832	0.512	4,26.870	1.487	0.234	4,33.398	1.738	0.165
	GT-Gi								
	Lever contacts			Probability lever			Latency lever		
	DF	F	p	DF	F	p	DF	F	p
Treatment	1,29.676	0.474	0.497	1,29.756	1.380	0.249	1,29.580	1.184	0.285
Session	4,29.339	2.842	**<0.05**	4,29.754	4.161	**<0.05**	4,66.666	1.612	0.182
*Treatment*session*	4,29.339	0.388	0.816	4,29.754	0.061	0.993	4,66.666	1.205	0.317
	ST-no DREADD								
	Lever contacts			Probability lever			Latency lever		
	DF	F	p	DF	F	p	DF	F	p
Treatment	1,19.424	0.065	0.801	1,16.672	0.200	0.661	1,16.238	0.079	0.782
Session	4,56.329	8.195	**<0.01**	4,46.156	18.797	**<0.01**	4,20.367	14,434	**<0.01**
*Treatment*session*	4,56.239	0.638	0.638	4,46.156	0.840	0.507	4,20.367	1.100	0.383
	GT-no DREADD								
	Lever contacts			Probability lever			Latency lever		
	DF	F	p	DF	F	p	DF	F	p
Treatment	1,13.133	4.440	0.055	1,17.211	3.680	0.072	1,18.443	3.223	0.089
Session	4,27.745	3.580	**<0.05**	4,45.408	3.928	**<0.01**	4,28.649	3.648	**<0.05**
*Treatment*session*	4,27.745	2.663	0.053	4,45.408	2.865	**<0.05**	4,28.649	3.475	**<0.05**

Table S2. Acquisition of Pavlovian conditioned approach during PavCA Sessions 1-5: magazine-directed behaviors.

	Magazine-directed behaviors (Goal-tracking)								
	ST-Gq								
	Magazine entries			Probability magazine			Latency magazine		
	DF	F	p	DF	F	p	DF	F	p
Treatment	1,23.121	3.333	0.081	1,26.890	3.097	0.090	1,26.238	3.305	0.081
Session	4,22.146	12.299	**<0.05**	4,40.812	13.489	**<0.01**	4,42.943	10.076	**<0.01**
*Treatment*session*	4,22.146	1.968	0.135	4,40.812	2.993	**<0.05**	4,42.943	2.013	0.110
	GT-Gq								
	Magazine entries			Probability magazine			Latency magazine		
	DF	F	p	DF	F	p	DF	F	p
Treatment	1,10.820	0.744	0.407	1,9.529	0.180	0.681	1,10.516	0.150	0.706
Session	4,11.690	18.267	**<0.01**	4,22.183	29.082	**<0.01**	4,15.998	31.383	**<0.01**
*Treatment*session*	4,11.690	0.495	0.740	4,22.183	0.210	0.930	4,15.998	0.238	0.913
	ST-Gi								
	Magazine entries			Probability magazine			Latency magazine		
	DF	F	p	DF	F	p	DF	F	p
Treatment	1,12.252	0.363	0.558	1,14.596	0.202	0.660	1,14.197	0.729	0.407
Session	4,14.652	3.461	**<0.05**	4,25.325	5.141	**<0.01**	4,21.601	5.225	**<0.01**
*Treatment*session*	4,14.652	0.765	0.565	4,25.325	0.759	0.561	4,21.601	0.751	0.568
	GT-Gi								
	Magazine entries			Probability magazine			Latency magazine		
	DF	F	p	DF	F	p	DF	F	p
Treatment	1,29.689	0.015	0.902	1,31.280	0.300	0.588	1,31.044	0.155	0.697
Session	4,39.931	21.667	**<0.01**	4,52.002	31.364	**<0.01**	4,47.028	30.693	**<0.01**
*Treatment*session*	4,39.931	0.296	0.879	4,52.002	0.342	0.849	4,47.028	0.937	0.937
	ST-no DREADD								
	Magazine entries			Probability magazine			Latency magazine		
	DF	F	p	DF	F	p	DF	F	p
Treatment	1,18.485	0.042	0.840	1,18.503	0.903	0.354	1,20.538	1.087	0.309
Session	4,32.474	2.128	0.100	4,35.919	2.612	0.051	4,35.722	3.220	**<0.05**
*Treatment*session*	4,32.474	1.111	0.368	4,35.919	0.443	0.777	4,35.722	0.447	0.773
	GT-no DREADD								
	Magazine entries			Probability magazine			Latency magazine		
	DF	F	p	DF	F	p	DF	F	p
Treatment	1,14.876	0.748	0.401	1,15.127	0.094	0.763	1,15.061	0.078	0.784
Session	4,24.330	14.599	**<0.01**	4,31.623	14.955	**<0.01**	4,23.690	12.976	**<0.01**
*Treatment*session*	4,24.330	1.538	0.223	4,31.623	2.040	0.113	4,23.690	1.730	0.177

Table S3. PavCA rescreening (Sessions 6-10) vs. PavCA test (Sessions 11-16): lever-directed behaviors.

	Lever-directed behaviors (Sign-tracking)								
	ST-Gq								
	Lever contacts			Probability lever			Latency lever		
	DF	F	p	DF	F	p	DF	F	p
Treatment	1,23	8.533	**<0.05**	1,23	21.366	**<0.01**	1,23	12.327	**<0.05**
Session	1,23	7.884	**<0.05**	1,23	11.196	**<0.05**	1,23	17.735	**<0.01**
*Treatment*session*	1,23	3.072	0.093	1,23	9.214	**<0.05**	1,23	6.526	**<0.05**
	GT-Gq								
	Lever contacts			Probability lever			Latency lever		
	DF	F	p	DF	F	p	DF	F	p
Treatment	1,10	0.415	0.534	1,10	0.261	0.621	1,10	0.164	0.694
Session	1,10	0.081	0.782	1,10	0.062	0.808	1,10	0.508	0.492
*Treatment*session*	1,10	0.014	0.908	1,10	0.008	0.929	1,10	0.003	0.957
	ST-Gi								
	Lever contacts			Probability lever			Latency lever		
	DF	F	p	DF	F	p	DF	F	p
Treatment	1,12	0.683	0.425	1,12	0.135	0.720	1,12	0.389	0.545
Session	1,12	1.651	0.223	1,12	0.441	0.519	1,12	2.553	0.136
*Treatment*session*	1,12	0.622	0.446	1,12	0.028	0.871	1,12	0.471	0.505
	GT-Gi								
	Lever contacts			Probability lever			Latency lever		
	DF	F	p	DF	F	p	DF	F	p
Treatment	1,30	1.597	0.216	1,30	1.350	0.254	1,30	2.160	0.152
Session	1,30	4.595	**<0.05**	1,30	5.164	**<0.05**	1,30	4.673	**<0.05**
*Treatment*session*	1,30	2.870	0.101	1,30	2.918	0.098	1,30	2.333	0.137
	ST-no DREADD								
	Lever contacts			Probability lever			Latency lever		
	DF	F	p	DF	F	p	DF	F	p
Treatment	1,15	1.322	0.268	1,15	0.089	0.769	1,15	0.014	0.909
Session	1,15	18.467	**<0.05**	1,15	4.797	**<0.05**	1,15	16.326	**<0.05**
*Treatment*session*	1,15	1.575	0.229	1,15	1.233	0.284	1,15	1.079	0.315
	GT-no DREADD								
	Lever contacts			Probability lever			Latency lever		
	DF	F	p	DF	F	p	DF	F	p
Treatment	1,13	0.040	0.845	1,13	0.001	0.974	1,13	0.014	0.908
Session	1,13	1.663	0.220	1,13	1.927	0.188	1,13	2.977	0.108
*Treatment*session*	1,13	0.602	0.452	1,13	0.265	0.616	1,13	0.000	0.992

Table S4. PavCA rescreening (sessions 6-10) vs. PavCA test (sessions 11-16): magazine-directed behaviors.

	Magazine-directed behaviors (Goal-tracking)								
	ST-Gq								
	Magazine entries			Probability magazine			Latency magazine		
	DF	F	p	DF	F	p	DF	F	p
Treatment	1,23	6.277	**<0.05**	1,23	6.674	**<0.05**	1,23	8.696	**<0.05**
Session	1,23	0.056	0.815	1,23	0.222	0.642	1,23	0.060	0.808
*Treatment*session*	1,23	3.518	0.073	1,23	5.323	**<0.05**	1,23	5.947	**<0.05**
	GT-Gq								
	Magazine entries			Probability magazine			Latency magazine		
	DF	F	p	DF	F	p	DF	F	p
Treatment	1,10	0.574	0.466	1,10	0.001	0.982	1,10	0.064	0.805
Session	1,10	0.078	0.786	1,10	0.003	0.957	1,10	1.815	0.208
*Treatment*session*	1,10	0.460	0.513	1,10	0.609	0.453	1,10	0.009	0.924
	ST-Gi								
	Magazine entries			Probability magazine			Latency magazine		
	DF	F	p	DF	F	p	DF	F	p
Treatment	1,12	1.116	0.312	1,12	0.439	0.520	1,12	0.046	0.834
Session	1,12	6.038	**<0.05**	1,12	7.279	**<0.05**	1,12	5.538	**<0.05**
*Treatment*session*	1,12	2.502	0.140	1,12	2.462	0.143	1,12	2.184	0.165
	GT-Gi								
	Magazine entries			Probability magazine			Latency magazine		
	DF	F	p	DF	F	p	DF	F	p
Treatment	1,30	0.459	0.503	1,30	3.271	0.081	1,30	3.416	0.074
Session	1,30	1.103	0.302	1,30	1.124	0.298	1,30	5.187	**<0.05**
*Treatment*session*	1,30	1.842	0.185	1,30	1.801	0.190	1,30	2.761	0.107
	ST-no DREADD								
	Magazine entries			Probability magazine			Latency magazine		
	DF	F	p	DF	F	p	DF	F	p
Treatment	1,15	0.352	0.562	1,15	0.430	0.522	1,15	0.347	0.564
Session	1,15	2.447	0.139	1,15	2.851	0.112	1,15	0.784	0.390
*Treatment*session*	1,15	1.356	0.262	1,15	1.211	0.289	1,15	0.482	0.498
	GT-no DREADD								
	Magazine entries			Probability magazine			Latency magazine		
	DF	F	p	DF	F	p	DF	F	p
Treatment	1,13	0.490	0.496	1,13	0.373	0.552	1,13	0.237	0.634
Session	1,13	0.198	0.664	1,13	0.025	0.876	1,13	0.428	0.525
*Treatment*session*	1,13	0.101	0.756	1,13	0.060	0.810	1,13	0.000	0.986

Table S5. Acquisition of sign-tracking behavior during PavCA Sessions 1-3: lever-directed behaviors.

	Lever-directed behaviors (Sign-tracking)								
	ST-Gq								
	Lever contacts			Probability lever			Latency lever		
	DF	F	p	DF	F	p	DF	F	p
Treatment	1,12.377	4.080	0.066	1,12,137	0.411	0.411	1,12.402	1.481	0.246
Session	2,13.246	17.459	**<0.05**	2,15.117	29.102	**<0.01**	2,13.358	23.444	**<0.01**
*Treatment*session*	2,13.246	0.014	0.986	2,15.117	0.179	0.838	2,13.358	0.636	0.545
	GT-Gi								
	Lever contacts			Probability lever			Latency lever		
	DF	F	p	DF	F	p	DF	F	p
Treatment	1,11.728	4.607	0.054	1,8.748	5.054	0.052	1,10.028	5.116	**<0.05**
Session	2,18.000	3.360	**<0.05**	2,16.264	0.655	0.533	2,16.333	1.715	0.211
*Treatment*session*	2,18.000	0.957	0.403	2,16.264	0.143	0.868	2,16.333	0.724	0.500

Table S6. Acquisition of sign-tracking behavior during PavCA Sessions 1-3: magazine-directed behaviors.

	Magazine-directed behaviors (Goal-tracking)								
	ST-Gq								
	Magazine entries			Probability magazine			Latency magazine		
	DF	F	p	DF	F	p	DF	F	p
Treatment	1,12.090	1.382	0.262	1,13.564	1.162	0.300	1,13.282	1.171	0.299
Session	2,13.611	4.155	**<0.05**	2,24.414	1.696	0.204	2,24.046	2.422	0.110
*Treatment*session*	2,13.611	0.480	0.629	2,24.414	0.523	0.599	2,24.046	0.697	0.508
	GT-Gi								
	Magazine entries			Probability magazine			Latency magazine		
	DF	F	p	DF	F	p	DF	F	p
Treatment	1,10.277	3.810	0.079	1,9.381	4.416	0.064	1,9.460	4.983	0.051
Session	2,18.000	9.671	**<0.05**	2,12.030	16.367	**<0.01**	2,11.614	15.136	**<0.05**
*Treatment*session*	2,18.000	2.501	0.110	2,12.030	1.832	0.202	2,11.614	1.533	0.256

Table S7. Session 3 vs. Session 6 of PavCA training: lever-directed behaviors.

	Lever-directed behaviors (Sign-tracking)								
	ST-Gq								
	Lever contacts			Probability lever			Latency lever		
	DF	F	p	DF	F	p	DF	F	p
Treatment	1,12	0.028	0.870	1,12	0.142	0.713	1,12	0.039	0.847
Session	1,12	0.244	0.630	1,12	0.163	0.694	1,12	0.164	0.692
*Treatment*session*	1,12	2.244	0.160	1,12	0.007	0.937	1,12	0.007	0.934
	GT-Gi								
	Lever contacts			Probability lever			Latency lever		
	DF	F	p	DF	F	p	DF	F	p
Treatment	1,8	23.653	**<0.01**	1,8	22.304	**<0.01**	1,8	19.311	**<0.05**
Session	1,8	6.706	**<0.05**	1,8	10.769	**<0.05**	1,8	9.333	**<0.05**
*Treatment*session*	1,8	3.144	0.114	1,8	3.276	0.108	1,8	2.777	0.134

Table S8. Session 3 vs. Session 6 of PavCA training: magazine-directed behaviors.

	Magazine-directed behaviors (Goal-tracking)								
	ST-Gq								
	Magazine entries			Probability magazine			Latency magazine		
	DF	F	p	DF	F	p	DF	F	p
Treatment	1,12	0.558	0.470	1,12	0.306	0.590	1,12	0.617	0.448
Session	1,12	1.134	0.308	1,12	0.339	0.571	1,12	1.063	0.323
*Treatment*session*	1,12	0.032	0.861	1,12	0.059	0.812	1,12	0.000	0.987
	GT-Gi								
	Magazine entries			Probability magazine			Latency magazine		
	DF	F	p	DF	F	p	DF	F	p
Treatment	1,8	1.876	0.208	1,8	4.878	0.058	1,8	3.061	0.118
Session	1,8	1.178	0.309	1,8	1.385	0.273	1,8	0.441	0.525
*Treatment*session*	1,8	13.131	**<0.01**	1,8	6.362	**<0.05**	1,8	7.785	**<0.05**

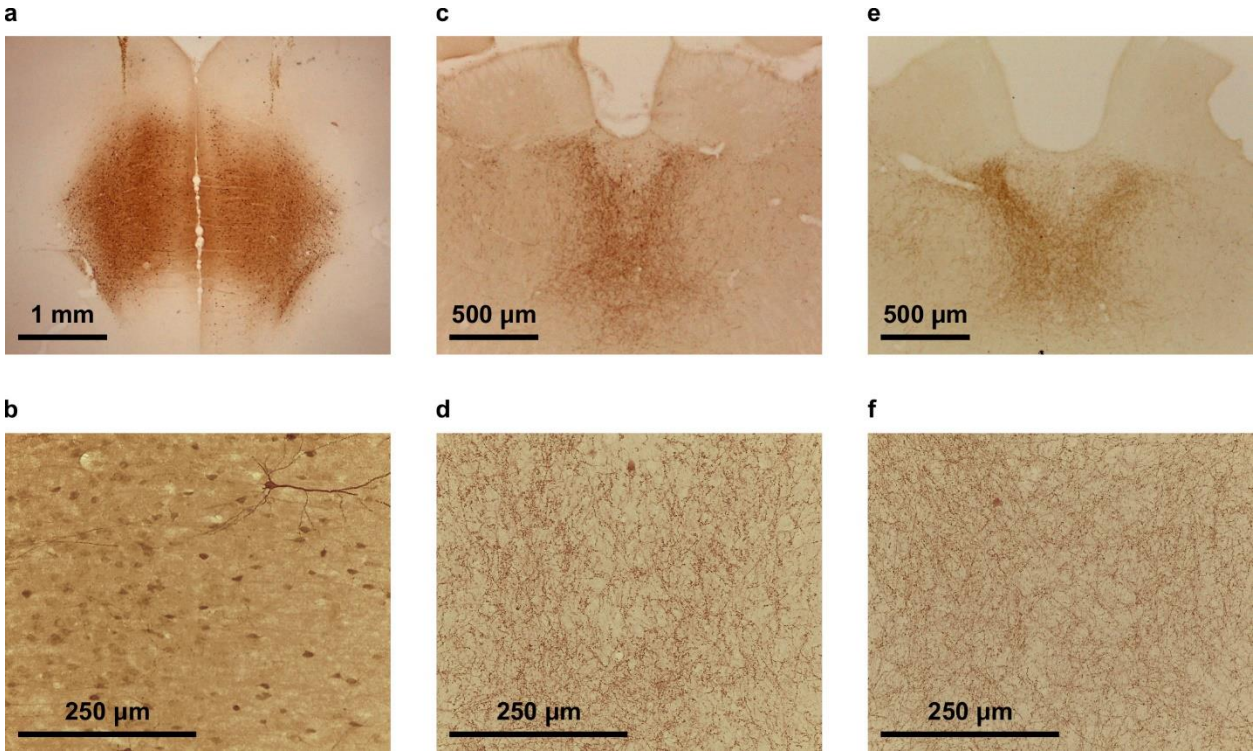

Figure S1. Representative photomicrographs of mCherry expression. a,b) Photomicrographs representing mCherry expression in the pyramidal neurons of the PrL projecting to the PVT at (**a**) 2.5x magnification and (**b**) 20x magnification. **c,d**) Photmicrographs of mCherry expression representing terminal fibers in the aPVT coming from the PrL at (**c**) 5x magnification and at (**d**) 20x magnification. **e,f**) Photomicrographs of mCherry expression representing terminal fibers in the aPVT coming from the PrL at (**e**) 5x magnification and (**f**) 20x magnification.

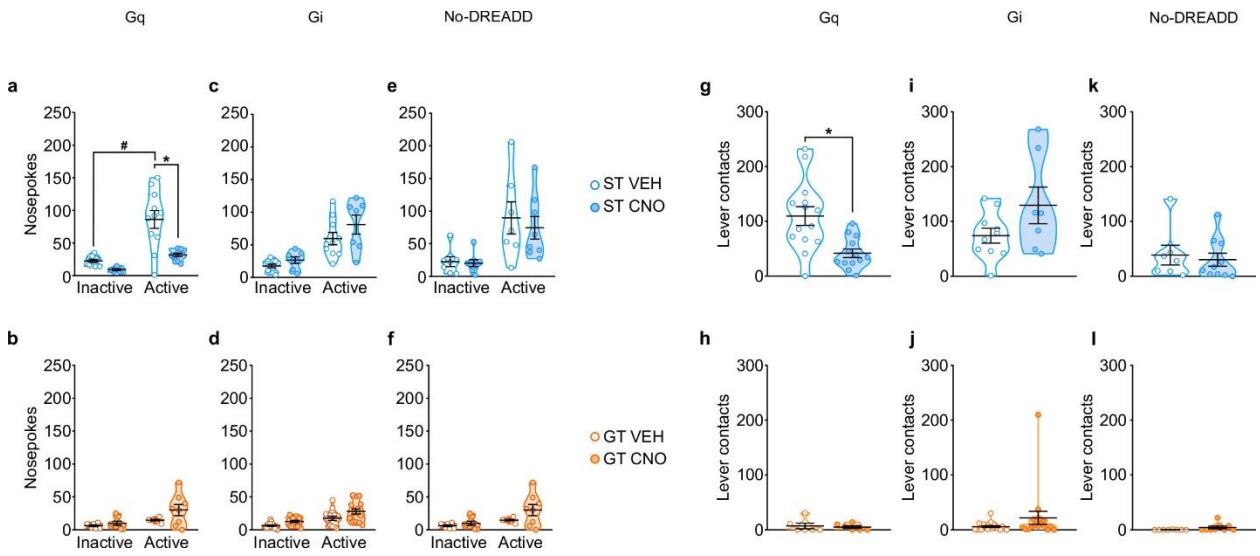

Figure S2. Chemogenetic stimulation of the PrL-PVT decreases the conditioned reinforcing properties of a reward-paired cue in sign-trackers. Data are expressed as individual data points with mean ± SEM plotted on violin plots. **a-f**) Noespokes into the inactive and active ports during conditioned reinforcement. **a,b**) Relative to VEH controls, administration of CNO (3 mg/kp, i.p.) significantly decreased nosepokes into the active port for (**a**) ST-Gq rats (*p<0.05 vs. VEH; #p<0.05 vs. Inactive), but not (**b**) GT-Gq rats. **c,d**) CNO-induced inhibition of the PrL-PVT circuit did not affect nosepokes in (**c**) ST-Gi or (**d**) GT-Gi rats. **e,f**) CNO administration did not affect nosepokes in non-DREADD expressing (**e**) STs or (**f**) GTs. **g-l**) Lever contacts during conditioned reinforcement. **g,h**) Relative to VEH controls, administration of CNO (3 mg/kp, i.p.) significantly decreased lever contacts for (**g**) ST-Gq rats (*p<0.05 vs. VEH), but not (**h**) GT-Gq rats. **i,j**) CNO-induced inhibition of the PrL-PVT circuit did not affect lever contacts in (**i**) ST-Gi or (**j**) GT-Gi rats. **k,l**) CNO administration did not affect lever contacts in non-DREADD expressing (**k**) STs or (**l**) GTs.

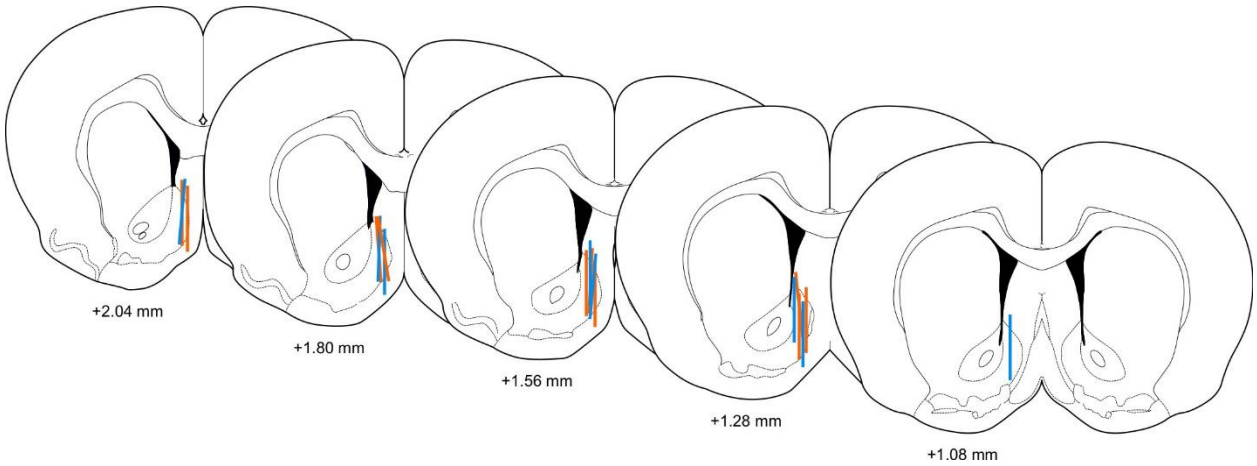

Figure S3. Microdialysis probe placement. Representative drawing of coronal sections of the brain showing the placement of microdialysis probes in the nucleus accumbens shell. The bars indicate the area of collection for STs (blue) and GTs (orange). Numbers indicate the approximate distance of the coronal slice relative from bregma.